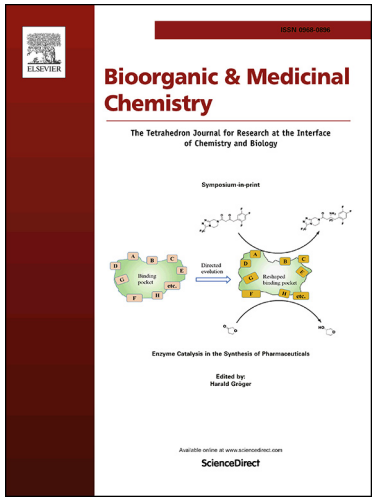

Design, synthesis, and evaluation of novel L-phenylglycine derivatives as potential PPARγ lead compounds

Liu Jinyu, Su Xiaoyan, Li Huachong, Fan Li, Li Yuanyuan, Tang Xuemei, Yan Jufang, Chen xin, Chen Feifei, Liu Jie, Yang Dacheng

PII: S0968-0896(17)32494-X
DOI: https://doi.org/10.1016/j.bmc.2018.07.005
Reference: BMC 14442

To appear in: *Bioorganic & Medicinal Chemistry*

Received Date: 29 December 2017
Revised Date: 13 June 2018
Accepted Date: 4 July 2018

Please cite this article as: Jinyu, L., Xiaoyan, S., Huachong, L., Li, F., Yuanyuan, L., Xuemei, T., Jufang, Y., xin, C., Feifei, C., Jie, L., Dacheng, Y., Design, synthesis, and evaluation of novel L-phenylglycine derivatives as potential PPARγ lead compounds, *Bioorganic & Medicinal Chemistry* (2018), doi: https://doi.org/10.1016/j.bmc.2018.07.005

Design, synthesis, and evaluation of novel L-phenylglycine derivatives as potential PPARγ lead compounds

Liu Jinyu [a,†], Su Xiaoyan [a,†], Li Huachong [a], Fan Li [a,*], Li Yuanyuan [a],Tang Xuemei [b], Yan Jufang [c], Chen xin [c], Chen Feifei [a], Liu Jie [a], Yang Dacheng [a,*]

[a] *Institute of Bioorganic and Medicinal Chemistry, Key Laboratory of Applied Chemistry of Chongqing Municipality, School of Chemistry and Chemical Engineering, Southwest University, Chongqing 400715, PR China.*

[b] *School of Life Science, Southwest University, Chongqing 400715, China*

[c] *Drug Screening Center, Chengdu Di Ao Pharmaceutical Group Co., Ltd., Chengdu 610041, China*

[†] Liu Jinyu and Su Xiaoyan have identical contribution to this work

Abstract: In accordance with the structural characteristics of thiazolidinedione drugs and highly bioactive tyrosine derivatives, we tentatively designed the L-phenylglycine derivatives **TM1** and **TM2** based on basic principles of drug design and then synthesized them. The *in vitro* screening of peroxisome proliferator-activated receptor gamma (PPARγ) activated activity, α-glucosidase inhibitory and dipeptidyl peptidase-4 inhibitory activities showed that the novel molecule **M5** had efficient PPAR response element (PPRE) activated activity (PPRE relative activity 105.04% at 10 μg·mL^{-1} compared with the positive control pioglitazone, with 100% activity). Therefore, **M5** was selected as the hit compound from which the **TM3** and **TM4** series of compounds were further designed and synthesized. Based on the PPRE relative activities of **TM3** and **TM4**, we discovered another new molecule, **TM4h**, which had the strongest PPRE relative activity (120.42% at 10 μg·mL^{-1}). In addition, the concentration-dependent activity of the highly active compounds was determined by assaying their half-maximal effective concentration (EC_{50}) values. The molecular physical parameter calculation and the molecular toxicity prediction were used to theoretically evaluate the lead-likeness and safety of the active compounds. In conclusion, we identified a potential PPARγ lead molecule and developed a tangible strategy for antidiabetic drug development.

Keywords: Diabetes mellitus; L-Phenylglycine; Tyrosine derivatives; Thiazolidinediones; Peroxisome proliferator-activated receptor; Dipeptidyl peptidase-4; *α*-Glucosidase

1. Introduction

Diabetes mellitus (DM) is an endocrine and metabolic disease, which has become the third most common non-infectious chronic disease after cardiovascular diseases and tumors. The Global Report on Diabetes published by World Health Organization in 2016 reported that there were approximately 422 million adults with DM worldwide, which will reach 592 million by 2035, and 90–95% are expected to be patients with type 2 diabetes mellitus (T2DM) [1]. T2DM (formerly called non-insulin-dependent or adult-onset diabetes) results from the body's ineffective use of insulin [1], characterized especially by insulin resistance [1]. T2DM can cause hypertension, diabetic retinopathy, and other chronic complications that lead to an increase in mortality [2]. Drugs currently used for the treatment of T2DM include insulin sensitizers (e.g., pioglitazone), insulin secretagogues (e.g., sulfonylureas), aldose reductase inhibitors (e.g., acarbose), dipeptidyl peptidase-4 (DPP-4) inhibitors (e.g., sitagliptin), sodium-glucose cotransporter (SGLT2) inhibitors (e.g., canagliflozin), and glucagon-like peptide-1 (GLP-1) receptor agonists (e.g., liraglutide) [1]. Although these drugs have clearly made outstanding contributions to the treatment of T2DM, the side effects caused by long-term use or high-dose administration has encouraged the continued search for novel T2DM drugs, which has attracted the attention of drug development researchers.

Peroxisome proliferator-activated receptor gamma (PPARγ) is mainly responsible for the regulation of the transcription of insulin-responsive genes, which control the production, transmission, and utilization of glucose [3]. PPARγ is also the key decisive factor controlling the development of adipocytes [4]. Of note, anti-diabetic drugs inhibit obesity-linked phosphorylation of PPARγ by cyclin-dependent kinase 5 (CDK5) [5]. PPARγ agonists are insulin sensitizers, and clinical drugs in this class include thiazolidine-2,4-dione (TZD) small molecule compounds such as rosiglitazone and pioglitazone [6]. Although TZDs have resulted in a significant breakthrough in the treatment of T2DM, their long-term use and high-dose administration may also lead to weight gain, edema, liver injury, and other side effects [7], which limited their clinical application. Thus, the development of high-efficacy and low-toxicity non-TZD PPARγ agonists has become a goal of researchers in this field. The study of non-TZD PPARγ agonists has revealed that several natural amino acids including phenylalanine, leucine, and histidine exert blood glucose-reducing effects [8] and numerous phenylalanine derivatives [9,10] (e.g., nateglinide) and tyrosine derivatives [11] (e.g., farglitazar, GW409544, and GW1929) have excellent PPARγ activated activity. Farglitazar, a classical tyrosine derivative, is also a strong PPARγ agonist [12]. Unfortunately, farglitazar was not successful in phase III

trials because of its adverse events such as angioneurotic edema [13]. Nonetheless, the studies mentioned above provided insights into the development of non-TZD PPARγ agonists with higher potency and lower toxicity than the existing agents.

A structural analysis of some TZDs (rosiglitazone, pioglitazone, and troglitazone) and tyrosine derivatives (GW409544, farglitazar, and GW1929) [14,15] (Scheme 1) revealed that PPARγ agonists typically include a hydrophilic group attached to the aromatic ring, a linker, and a hydrophobic group [14,16]. Unlike TZDs, tyrosine derivatives have a lipophilic group derived from the α-amino group, which is believed to improve the PPARγ affinity of farglitazar compared with that of TZDs [15]. The above information indicates that the target molecule should contain the required pharmacophore for PPARγ agonists as well as the previously mentioned lipophilic groups and, accordingly, we tentatively designed molecule **A** (Scheme 1).

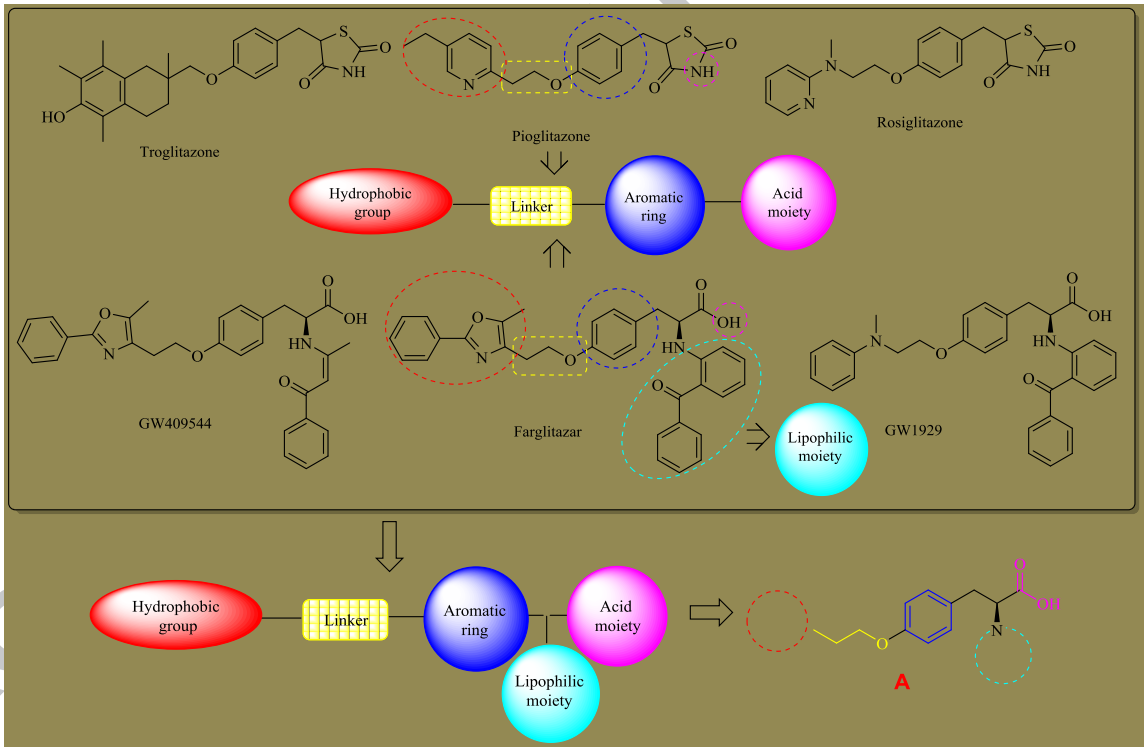

Scheme 1. Designed molecules inspired by thiazolidine-2,4 -diones (TZDs) and tyrosine derivatives.

Molecule **A** is a structural derivative of tyrosine. The truncation of the CH_2 of **A** converted it into a phenylglycine derivative, which has been used widespreadly, for instance, the chlorophenylglycine derivatives are used in the synthesis of penicillin and cephalosporin derivatives [17] and the *D-p*-hydroxy -phenylglycine is a side chain of semi-synthetic *β*-lactam antibiotics [18]. However, there are few reports on the integration of a phenylglycine unit into antidiabetic drug molecules. Therefore, we hypothesized that

an antidiabetic molecule with high potency and low toxicity would be obtained by changing the tyrosine residue to a phenylglycine residue. Thus, we further designed molecule **B** from **A** (Scheme 2).

It is well known that the ligand-binding domain (LBD) of PPAR is a large, Y-shaped site surrounded by 13 α-helices and a small four-stranded *β*-sheet [13]. Ligands usually adopt a U-shaped conformation when binding to the LBD of PPARγ [19]. Most PPARγ agonists contain a flexible alkyl ether linkage to enhance their binding to receptors [20]. Khanna et al. shifted alkyl ether bond from *para*-site to *meta*-site [21] and Suh et al. replaced the flexible linker at the *meta*-site with a rigid linker [18], which resulted in strong PPARγ activated activity. Thus, we not only changed the location of the alkyl ether group of the PPARγ agonist but also performed rigidity-flexibility exchange. Consequently, we changed the flexible alkyl ether bond of **B** in the *para*-site into an alkyl amide in the *meta*-site to obtain molecule **C** (Scheme 2).

The mechanism of action of TZD drugs indicates that either the aliphatic group or the heterocyclic aryl could be selected as the hydrophobic part of target molecule because of the large binding cavity of the receptor [22]. We used fragment-based drug design and, therefore, drug molecular fragments or drug-like molecular fragments were given prior consideration as hydrophobic R^1 groups of the target molecules. Therefore, the selected fragment R^1 comprised of sulfamethoxazole (antibacterial drug), benzimidazole (the fragments of omeprazole and rabeprazole) and phthalimide (derivatives thereof have anti-inflammatory [23], antibacterial [24], and antitumor [25] activities). We also chose benzyloxycarbonyl (Cbz), an ordinary and readily removable group, as the lipophilic group of the target compounds. In order to get more information about structure-activity relationships (SARs), the acidic COOH of the target molecules was converted into neutral $COOCH_3$. Based on the above requirements, we designed and synthesized the target molecules **TM1** and **TM2** (Scheme 2) with L-phenylglycine as the basic skeleton, and then assessed their PPARγ activated activity.

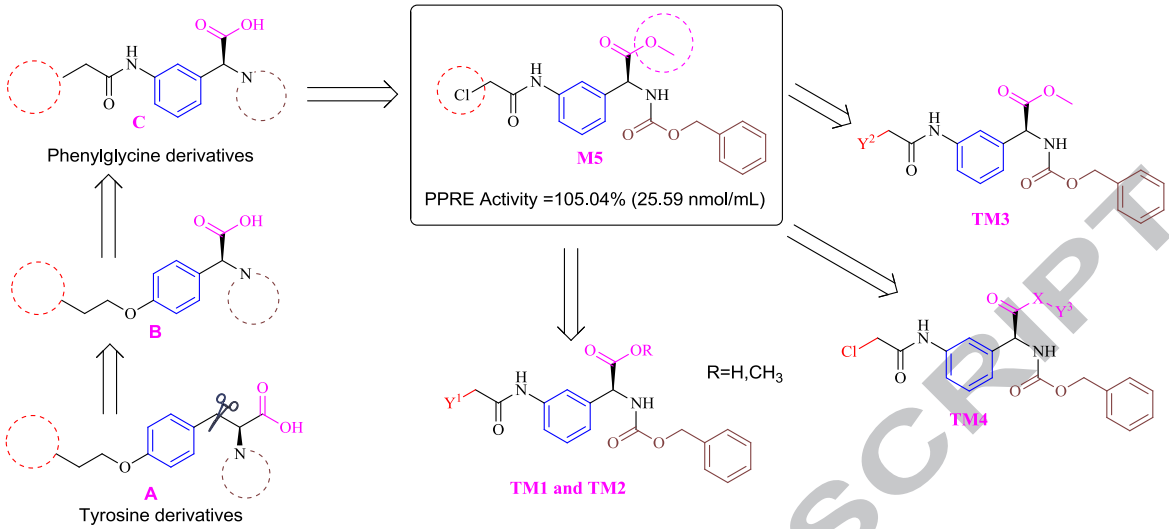

Scheme 2. Design of target molecules **TM1**–**TM4**.

Preliminary activity screening showed that both **TM1** and **TM2** exhibited poor PPARγ activated activities, whereas the intermediate **M5** (Scheme 2) exhibited better PPARγ activated activity (the PPRE relative activity was 105.04% at 10 μg·mL^{-1}). Therefore, we designed and synthesized **TM3** and **TM4** by altering both the carboxyl-terminal and chlorine atom of **M5**. The biological activity screening of **TM3** and **TM4** revealed that compound **TM4h** had the highest activity, which not only confirmed the correctness of our molecule design, but also provided a new direction and foundation for subsequent research.

2. Results and discussion

2.1 Synthesis

2.1.1 Synthesis of **TM1** and **TM2**

TM1 and **TM2** can be structurally divided into an *L*-3-aminophenylglycine moiety and a hydrophobic moiety linked to the aromatic amine group; thus, we designed four synthetic routes (Scheme 3).

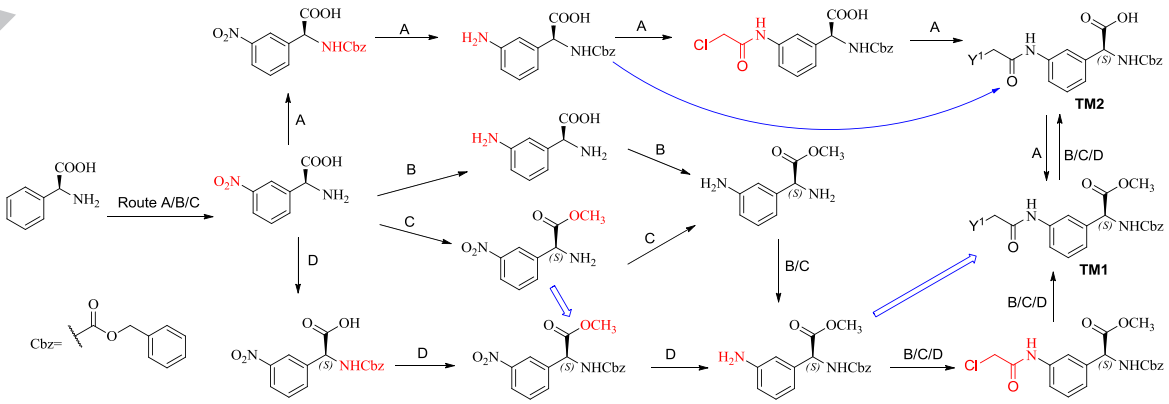

Scheme 3. Synthetic routes of designed target compounds **TM1** and **TM2**

Route A consists of six steps: nitration of phenylglycine, protection of the α-amino group, reduction of the nitro group, acetylation of the amino group at the benzene ring, substitution of the chlorine atom, and methyl esterification of the carboxyl group. Route A had the shortest steps and, thus, was our initial preference. However, we found that although the crude **TM2** product could be successfully obtained after the step substituting the chlorine atom, purification of the product was difficult owing to the numerous side reactions and its poor solubility. In addition, it was difficult to convert some **TM2** compounds to their **TM1** counterpart, owing to their poor solubility. The reaction for route B was similar to that of route A, except for an extra step (hydrolysis of the methyl ester) and the different order of reactions. Route B is a typical step-by-step synthesis method and all the intermediates and target molecules can be obtained theoretically. However, in this route, the raw material and product of the nitro reduction are often covered in zinc powder, which results in a long reduction time, incomplete reduction, low extraction and separation efficiency, and extremely low yield. Route C is similar to route B, which contains the same unit reaction, but the formation of methyl ester is performed prior to the reduction of nitro. Route C overcame the problem associated with a reduction of the nitro in route B, but two amino groups still exist in the molecule. This indicates that benzylamine would also be protected in the step protecting α-amino with Cbz, making selective protection difficult. Although route D still uses L-phenylglycine as the raw material, Cbz protection of α-amino group and methyl esterification of carboxyl group are carried out before nitro group reduction. This process not only addresses the reduction issues but also selectively protects amino group easily and provides essential intermediates and target molecules. Therefore, route D is a feasible synthetic route in theory.

We previously reported the nitration of phenylglycine and the subsequent modification of the α-amino group [26~28] using experimental methods well-developed by our laboratory and the overall yield of both steps was over 80%. The combination system of Alcohol (ROH)/thionyl chloride ($SOCl_2$) is usually used as the reagent for esterification of amino acids in our laboratory [29] to deliver an alkyl ester with high purity and a satisfactory yield. We also adopted $SOCl_2$/methanol (MeOH) as the reaction reagent in the synthesis of **M2** to **M3** and found that this simple and convenient process generated the corresponding alkyl ester at a very high yield (over 85%). The significant step in the synthesis of the target products **TM1** and **TM2** is the reduction of nitro group (the synthesis of **M4**), which requires both the successful reduction of $-NO_2$ and prevention of side reactions on the $-CO_2CH_3$ and -Cbz group. We attempted reduction reactions using 80% hydrazine hydrate, Zn/ammonium chloride (NH_4Cl)/acetic acid (HOAc), Zn/HOAc, Zn/NH_4Cl, and Zn/$CaCl_2$ and finally discovered that the Zn/NH_4Cl/HOAc reduction was the best. However, we identified an impurity close to the target molecule after repeated TLC analyses, which indicated that it would be very difficult to obtain a pure product using column chromatography alone. Additionally, prolonged exposure of the reduction product to air would oxidize it and, so, it is not efficient to purify **M4** just using column chromatography. We attempted the next chloroacetylation reaction with crude **M4** and, fortunately, found that the reaction proceeded smoothly, the purification was simple, and the total yield of both steps was approximately 50–70%. Thus, the large-scale synthesis of **M5** became practical, which provided a solid foundation for the synthesis of the target molecules **TM1** and **TM2**.

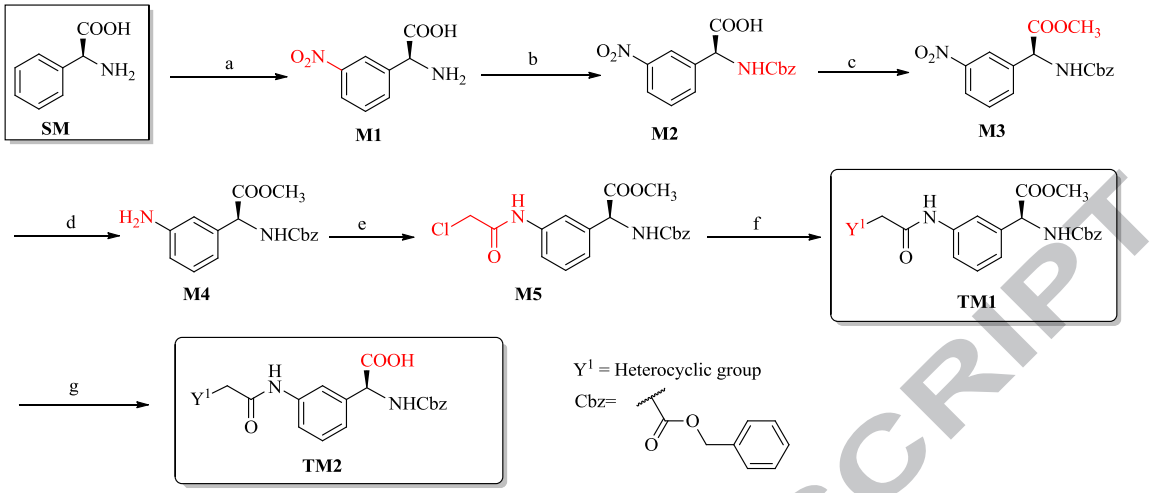

Scheme 4. Synthesis of **TM1** and **TM2**: **(a)** HNO_3, H_2SO_4, 85%; **(b)** benzyloxycarbonyloxysuccinimide, 10% K_2CO_3, acetone, 92%; **(c)** MeOH, $SOCl_2$, 83%; **(d)** Zn, NH_4Cl, MeOH; **(e)** 2-chloroacetyl chloride, K_2CO_3, acetone, 80%; **(f)** Y^1-H, K_2CO_3, DMF, 38% for **TM1a**, 75% for **TM1b**, 66% for **TM1c**, 73% for **TM1d**, and 85% for **TM1e**; **(g)** LiOH, THF; 10% HCl, 86% for **TM2a**, 83% for **TM2b**, 87% for **TM2c**, 95% or **TM2d**, and 90% for **TM2e**.

The synthesis of **TM1** through the reaction of **M5** with amine or thiophenol (Y^1-H) is a typical nucleophilic substitution, and the related experimental results are presented in the supporting information. The yields of **TM1b**–**TM1e** were above 60%, whereas that of **TM1a** was only 38.7%. This was attributed to the nucleophilicity of the nucleophile. Specifically, since the acidity of the N-H of phthalimide is greater than that of benzimidazole, the N-H of phthalimide is more likely to convert into a negative nitrogen ion under alkaline conditions. Therefore, **TM1b** exhibited a stronger reactivity and higher yield than **TM1c** did. *N*-Boc-piperazine and 2-mercaptobenzimidazole are both strong nucleophiles; however, 2-mercapto-benzimidazole is a planar molecule and the nucleophilic ability of the sulfur atom is stronger than that of the nitrogen atom and, therefore, the yield of **TM1e** was higher than that of **TM1d**. In addition, the NH_2 on the benzene ring of sulfamethoxazole was conjugated with the benzene ring bearing a strong electron-withdrawing group sulfonamide, which resulted in the poor nucleophilicity of NH_2 group and, thus, a low reaction rate. Furthermore, the relatively large molecular weight and poor solubility of **TM1a** made column chromatography difficult and, thus, **TM1a** was obtained with the lowest yield.

TM2 can conveniently be prepared by the hydrolyzing the corresponding **TM1**. Methyl ester is usually hydrolyzed under acidic or alkaline conditions. The -Cbz would likely be removed under strong acidic conditions, and the chiral molecules would probably undergo racemization under intense conditions and, therefore, **TM1** must be hydrolyzed under mild condition. By exploring various experimental conditions, we found that THF was used as the solvent, pH adjusted to 10–11 by LiOH, temperature was controlled between 16–25^{o}C, and the reaction was completed within 1 hour without racemization. The

experimental results are given in the supporting information.

2.1.2 Synthesis of **TM3** and **TM4**

The **TM3** and **TM4** series were the target molecules we further designed using **M5** as the hit molecule. **TM3** is a series of compounds derived from **M5** by the substitution of a chlorine atom and, therefore, they can be synthesized by conventional amidation and the substitution of heterocyclic amine. The former process requires the reaction of **M4** with the corresponding acyl chloride R^3CH_2COCl and the latter involves a nucleophilic substitution reaction between heterocyclic amines and **M5**. **TM4** is an alternative derivative of the carboxyl methyl ester of **M5**, which is similar to **M5** structurally and can be prepared using two synthetic routes. 1) Starting from **M2**, **TM4b–TM4h** were assembled by the esterification or amidation of a carboxyl group (converted to **M6**), followed by direct chloroacetylation of the amino group after the reduction of nitro group. 2) **TM4a** was generated through a two-step reaction between nitro reduction of **M2** (affording **M7**) and chloroacetylation of amino group. The synthetic route is shown in Scheme 5.

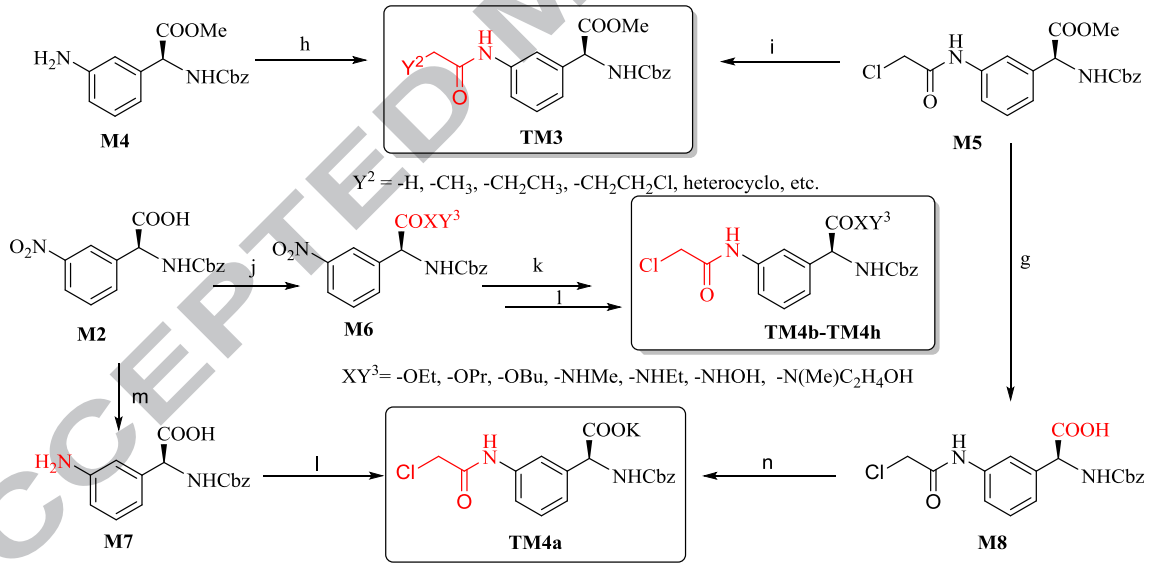

Scheme 5. Synthesis of **TM3** and **TM4**: **(h)** Y^2-acyl chloride, K_2CO_3, acetone, 65% for **TM3e**, 53% for **TM3f**, 51% for **TM3g**, 65% for **TM3h**, 62% for **TM3i**, and 52% for **TM3j**; **(i)** Y^2-H, K_2CO_3, DMF, 66% for **TM3a**, 55% for **TM3b**, 53% for **TM3c**, and 32% for **TM3d**; **(j)** H-XY^3, $SOCl_2$ or dicyclohexylcarbodiimide, 85% for **M6b**, 88% for **M6c**, 88% for **M6d**, 92% for **M6e**, 88% for **M6f**, 67% for **M6g**, and 86% for **M6h**; **(k)** Zn, NH_4Cl, MeOH; **(l)** 2-chloroacetyl chloride, K_2CO_3, acetone, 73% for **TM4a**, 65% for **TM4b**, 70% for **TM4c**, 62% for **TM4d**, 27% for **TM4e**, 46% for **TM4f**, 56% for **TM4g**, and 38% for **TM4h**; (**m**) Zn, $CaCl_2$, 85%; (**n**) K_2CO_3, DCM.

The results of the **TM3** preparation are shown in the supporting information. **TM3a–TM3d** were synthesized by the nucleophilic substitution reaction between **M5** and azoles with a yield of 32–66%. The yield of **TM3d** was only 32.7%, which was attributed to the steric hindrance of the *ortho*-methyl group.

The azoles used to prepare **TM3b** and **TM3c** contained resonance structures (Scheme 6), which include a plurality of reaction sites and, therefore, the purification of these products is not easy. In fact, we only separated the main target products while other isomers generated at other sites were not isolated. **TM3e**–**TM3i** were obtained by acylation of **M4** with different acyl chlorides, and the total yield of the two-step reaction was over 51%.

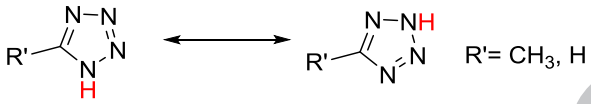

Scheme 6. Resonant structures of azoles used to prepare **TM3b** and **TM3c.**

The key synthetic step of the target products **TM4b**–**TM4h** is the synthesis of **M6**. As a derivative of **M2**, **M6** is prepared by esterification or amidation of the carboxyl group of **M2**. There are numerous methods for esterifying carboxyl groups including the carboxylic acid coupling method aided by dicyclo-hexylcarbodiimide (DCC) or 1-ethyl-3-(3-dimethylaminopropyl)carbodiimide (EDCI) [30]. We used the $SOCl_2$/ROH method previously used in our laboratory to produce **M6b**–**M6d** with high purity and excellent yield (85–92%) [29,31,32]. The general synthetic methods of amides include the reaction of acyl halides, mix acid anhydrides, acyl azides as well as active esters with amines. Although numerous methods are available for activating carboxylic function, we usually used a condensation reagent (such as carbodiimide and onium-type regents) to convert chiral amino acids into corresponding amides [30]. While the purification process is tedious, the yield is high, and racemization rarely occurs [30]. In this experiment, DCC was used as activation agent, and hydroxybenzotriazole (HOBt) was used as additive. The molar ratio of **M2**, DCC, HOBt, and base components was 1:1.2:1.2:1.2, and the yields of **M6e**–**M6h** were 67–92%. As shown in the supporting information, the yield of **M6e** was the highest (92.0%), which may be related to the small volume of methylamine while that of **M6g** was only 67.5%, mainly because there were two reaction sites in hydroxylamine hydrochloride.

The synthesis of **TM4b**–**TM4h** from **M6** required two steps, consisting of reduction of nitro group and acylation of the resulting amino group. Given the properties of amino acids, the reaction conditions were set as mild as possible to obtain high purity products without racemization, and the reaction yield was not the main priority. The characterization results of **TM4** derived from **M6** are presented in the supporting information. The yields of **TM4e** and **TM4h** were relatively low, which was thought to be the result of product loss during the repeated recrystallization steps.

The key step of the synthesis of **TM4a** is the production of **M7** from **M2.** Owing to the amphoteric properties of amino acids, we initially selected Zn/NH_4Cl/HOAc as the reducing reagent for **M2**. However, due to the high water solubility of **M7**, this lead to a low yield which prevented the effective separation of the product from the reaction mixture after adding excess water in the subsequent process. To improve the yield of **M7**, we systematically studid possible strategies and finally established the Zn/$CaCl_2$ reduction, and thus obtaining excellent yield with high purity (see supporting information). When we adopted the optimal procedure, the acylation of **M7** proceeded smoothly, and the preparative results of **TM4a** are shown in the supporting information.

2.2 SAR

2.2.1 SAR of TM1 and TM2

PPARs are a nuclear hormone receptor superfamily, comprised of three subtypes namely PPARα, PPARγ, and PPARδ [33,34]. Presently, the fibrate-type lipid-lowering drugs (such as fenofibrate) and certain insulin sensitizers sold on the market belong to PPARα and PPARγ agonists, respectively. PPARδ is involved in lipid transport and metabolism, but currently, there is no listed drug with PPARδ activity [35]. In the presence of ligands, the PPAR heterodimer, which contains the retinoid X receptor (RXR), regulates the transcription of target genes by binding to the PPRE in the promoter region of the target gene. Stimulation by endogenous ligands such as saturated or unsaturated fatty acids and arachidonic acid derivatives or exogenous blood lipid-reducing antidiabetic drugs initiate the PPAR response by acting as a molecular sensor and trans-activating the target genes. Therefore, PPRE is an effective tool for the evaluation of potential PPAR agonists. In this study, the antidiabetic activity of target molecules was assessed by assaying PPRE relative activity.

The *in vitro* PPRE relative activity of the target molecules (10 $\mu g \cdot mL^{-1}$) was evaluated using pioglitazone (0.78 $\mu g \cdot mL^{-1}$, 100%) as the positive control. As shown in Table 1, most molecules of the **TM1** and **TM2** series possessed weak PPRE relative activity at tested concentrations. However, **TM2a**, **TM2b**, and **TM2e** exhibited potent PPRE relative activity of 40.63 %, 39.93%, and 32.91%, respectively. The activity intensities indicated that the PPRE relative activity of the **TM2** series of compounds, which have a carboxyl group at the hydrophilic end, were more active than those of the corresponding **TM1** series compounds, which have a carboxylic acid methyl ester at the hydrophilic end. This may be related to the water solubility of these compounds and the presence of carboxyl groups.

Table 1

PPRE relative activity of **TM1**, **TM2**, and intermediates

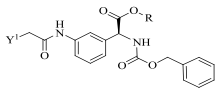

Compound	-Y[1]	-R	Concentration μg·mL^{-1}/μmol·L^{-1}	PPRE/%	
				Activity	Relative Activity*
M5	-Cl	-CH_3	10/25.59	**105.04**	**100.00**
TM1a	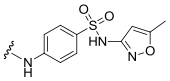	-CH_3	10/16.45	18.85	27.91
TM1b		-CH_3	10/19.94	11.92	14.56
TM1c		-CH_3	10/21.16	3.93	4.52
TM1d	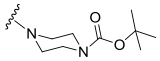	-CH_3	10/18.50	-8.27	-10.89
TM1e	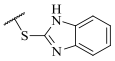	-CH_3	10/19.82	7.66	-9.41
M8	-Cl	-H	10/26.54	53.49	**49.10**
TM2a	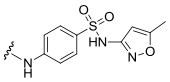	-H	10/16.84	40.63	**58.77**
TM2b		-H	10/20.51	39.93	**47.43**
TM2c	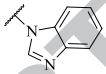	-H	10/21.81	3.85	4.30
TM2d	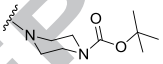	-H	10/18.99	21.43	27.49
TM2e	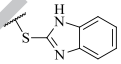	-H	10/20.38	32.91	**39.37**
Pioglitazone	/		0.78/2.19	100	

*The data in relative activity is the PPRE activity at the equal molar concentration (μmol·L^{-1}) converted by (PPRE/Conc.) ×24.36, and the value of PPRE is an average value of four measurements

The PPRE relative activity of **TM2** was stronger than that of **TM1**, which was consistent with our design idea. However, unexpectedly, the activity of **TM2** was not as potent as that of the intermediate, **M5** (methyl ester group), which exhibited higher potency than that of **M8** (carboxyl group). Therefore, we suggested that **M5** may be a novel PPARγ hit compound.

To predict the selectivity of the compounds, we further evaluated the inhibitory effects of **TM1**, **TM2**, and selected intermediates on α-glucosidase and DPP-4. α-Glucosidase retards the absorption of glucose in the intestinal tract, thereby delaying the peak postprandial blood glucose levels to control

excessive elevation. Currently marketed α-glucosidase inhibitors include voglibose, acarbose, and miglitol [36]. DPP-4 is a transmembrane serine protease that belongs to the proline oligopeptide family [37]. DPP-4 inhibitors, as the name suggests, inhibit the activity of DPP-4, leading to increased levels of glucagon-like peptide (GLP)-1 and gastric inhibitory peptide (GIP) [38]. These actions regulate the blood glucose and other indicators to achieve the goal of diabetes treatment. KR-62436, a DPP-4 inhibitor, was approved for clinical use by the US Food and Drug Administration (FDA) in 2007 [39,40]. As shown in Table 2, compared with the reference drugs, voglibose and KR-62436, the α-glucosidase and DPP-4 inhibitory activities of **TM1**, **TM2**, and their intermediates were extremely weak, showing that both **TM1** and **TM2** displayed good target specificity.

Table 2

α-Glucosidase and DPP-4 inhibitory activity of **TM1**, **TM2**, and selected intermediates*

Compd.	Concentration /μmol·L^{-1}	***α*-Glucosidase Inhibition /%**	**DPP-4 Inhibition /%**	**Compd.**	Concentration /μmol·L^{-1}	***α*-Glucosidase Inhibition /%**	**DPP-4 Inhibition /%**
M5	25.59	14 .63	16.12	**M8**	26.54	17.66	-17.33
TM1a	16.45	11.85	5.87	**TM2a**	16.84	8.89	11.10
TM1b	19.94	17.53	2.17	**TM2b**	20.51	17.83	-33.95
TM1c	21.16	2.91	-0.31	**TM2c**	21.81	0.99	-0.74
TM1d	18.50	15.46	-6.12	**TM2d**	18.99	13.69	5.26
TM1e	19.82	9.26	8.99	**TM2e**	20.38	12.58	-7.54
Voglibose	3.74	103.95	/	**KR-62436**	0.81	/	73.11

*The value of measured activities is an average value of four measurements.

2.2.2 SAR of TM3 and TM4

The proposed design of the **TM3** series of molecules included replacing the chlorine atoms in the **M5** molecule with different groups to investigate the effect of different groups on the biological activity. Therefore, azoles and simple groups with similar or slightly larger size as chlorine atom became preferred substituents in molecular design. It is reported that diazole derivatives have anti-inflammatory and antibacterial effects, and can regulate plant growth [41]. Tetrazole and its derivatives can be used to synthesize pesticides, medicines, photographic materials, and other substances [42]. We attempted to design and synthesize 10 derivatives of **TM3** by selecting diazole, tetrazoles, chlorine-free alkyl groups,

chloroalkyl and methoxy groups, as well as hydrogen atom to replace the chlorine atom in **M5** molecule. The PPRE relative activity of **TM3** was measured with pioglitazone as the positive control, and the results are presented in Table 3.

Table 3

PPAR response element (PPRE) relative activity of **TM3**.

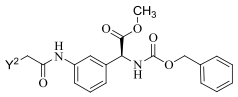

Compound	-Y^2	Concentration μg·mL^{-1}/μmol·L^{-1}	PPRE/%	
			Activity	Relative Activity*
M5	-Cl	10/25.59	**105.04**	**100.00**
TM3a	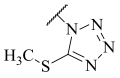	10/21.25	19.53	22.39
TM3b		10/22.81	14.45	15.43
TM3c		10/23.56	14.45	14.94
TM3d	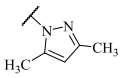	10/22.20	1.36	1.49
TM3e	-H	10/28.06	24.93	21.64
TM3f	-CH_3	10/27.00	18.28	16.49
TM3g	-C_2H_5	10/26.01	12.01	11.25
TM3h	-CH_2Cl	10/24.70	-3.55	-3.50
TM3i	-CH_2CH_2Cl	10/23.87	11.58	11.81
TM3j	-OCH_3	10/25.88	-17.07	-16.07
Pioglitazone	/	0.78/2.19	100	

*The data in relative activity is the PPRE activity at the equal molar concentration (μmol·L^{-1}) converted by (PPRE/Conc.) ×24.36, and the value of PPRE is an average value of four measurements

Table 3 shows that all compounds containing azole unit in **TM3** series exhibited weak PPRE relative activity (< 30%) at 10 μg·mL^{-1} in the following decreasing order of magnitude: **TM3a** > **TM3b** > **TM3c** > **TM3d**. The substitution of a chlorine atom with a hydrogen atom, methyl, and ethyl produced the following compounds with decreasing magnitude of activity: **TM3e** > **TM3f** > **TM3g**, which was possibly related to the alkyl volume. In contrast, the compounds with chloroalkyl group (**TM3h** and **TM3i**) or a methoxy group (**TM3j**), showed PPRE relative activity in the following decreasing order: **TM3i** > **TM3h** >

TM3j, which shows that the stronger the electron-withdrawing effect of the substituent, the weaker the PPRE relative activity of the corresponding molecule. However, because the changes described above did not result in a more active compound than **M5**, the Y^2 part of the molecule requires further investigation.

Based on the PPARγ activated activities of the **TM3** series, we decided to retain the chloroacetyl unit of **M5** and vary the methyl carboxylate moiety, which led to the design of the **TM4** series of molecules. Initially, a soluble potassium carboxylate (**TM4a**) with good solubility was designed, and then the homologs of the methyl ester, that is, the ethyl (**TM4b**), propyl (**TM4c**), and butyl (**TM4d**) esters were also designed. Furthermore, adopting the principle of drug design by converting the ester group into an amido, we further designed the target molecules **TM4e**–**TM4h**, corresponding to the amides of methylamine, ethylamine, hydroxylamine, and -N(Me)C_2H_4OH. After these eight target molecules were synthesized , their PPRE relative activities *in vitro* were assayed. The results presented in Table 4 showed that the PPRE relative activities of **TM4b**–**TM4g** were extremely weak while that of **TM4a** was 53.49%, but still weaker than that of **M5**. Fortunately, the PPRE relative activity of **TM4h** was 120.42%, not only stronger than that of pioglitazone, but also higher than the lead molecule **M5**. The activity of the **TM4** series showed that carboxyl terminus of phenylglycine derivatives could be either ester or amido group, and the other part of these molecules should contain a hydrophobic moiety, which is consistent with the structural characteristics of TZD and tyrosine derivatives.

Table 4

PPRE relative activity of **TM4**.

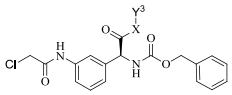

Compound	-XY^3	Concentration μg·mL^{-1}/μmol·L^{-1}	Relative PPRE/%	
			Activation	Activation*
TM4a	-O^-K^+	10/24.70	**53.49**	**52.75**
TM4b	-OEt	10/25.32	-24.83	-23.89
TM4c	-OPr	10/24.46	-17.14	-17.07
TM4d	-OBu	10/21.89	-5.01	-5.58
TM4e	-NHMe	10/26.33	-18.80	-17.39
TM4f	-NHEt	10/25.39	-20.13	-19.31
TM4g	-NHOH	10/26.19	-5.33	-4.96

TM4h	-N(Me)C_2H_4OH	10/23.59	**120.42**	**124.35**
Pioglitazone	/	0.78/2.19	100	

*The data in relative activity is the PPRE activity at the equal molar concentration (μmol·L^{-1}) converted by (PPRE/Conc.) ×24.36, and the value of PPRE is an average value of four measurements.

Based on the preliminary screening, we further evaluated the half-maximal effective concentration (EC_{50}) of **M5** and **TM4h** which were the most active among the designed molecules (Table 5).

Table 5

EC_{50} values of most active compounds.

Compound	EC_{50}(μmol·L^{-1})	Max Activated activity (%)	Max Conc. (μmol·L^{-1})
M5	22.39	178.74	25.59
TM4h	8.97	208.04	23.05
Pioglitazone	0.24	142.47	2.19

2.3 Lead-likeness and toxicity

2.3.1 Lead-likeness and toxicity prediction of TM1 and TM2 series

To predict the lead-likeness of the **TM1** and **TM2** series of compounds, we calculated their physicochemical parameters using the PLEXUS software provided by Eli Lilly and Co., and the results were given in Table 6. It is well known that the physicochemical properties of molecules are one of the factors that must be considered in selecting lead compounds. The cLogP is an important parameter describing the hydrophobic properties of compounds; the larger the cLogP, the better the hydrophobicity of the compound [43]. The topological polar surface area (tPSA) is the sum of the surfaces of polar atoms in a molecule. Presently, it is generally considered that a tPSA value ≤ 140 is best [44]. Table 6 shows that the cLogP values of the **TM1** series were generally much higher than those of the **TM2** series were, but the **TM2** series exhibited stronger PPRE relative activity. This observation indicates that the PPAR target protein maybe requires a better spatial matching rather than stronger lipophilicity. Table 6 also shows that the tPSA values of **TM2** series compounds are higher than those of **TM1** series, indicating that the higher the tPSA value of a compound, the stronger its interaction with the PPAR target protein. Therefore, the corresponding PPARγ activated activity of the compound with greater tPSA value is better than that of compounds with lower values.

Lipinski's rule of five (RO5) is an indicator of the oral bioavailability of compounds, involving molecular weight, cLogP, and the number of hydrogen bond donors (H-bond donors) or acceptors (H-bond

acceptors) [45]. The molecular weights of our compounds are all approximately 500, which essentially meet the requirements of RO5. The **TM2** molecules, having carboxyl groups as their hydrophilic end groups, have better water solubility, lower cLogP, and generally better activity than the **TM1** molecules. Both **TM1** and **TM2** series of molecules have H-bond acceptors and donors, accordingly, **TM2a**, with the largest number of H-bond acceptors (8) and donors (5), has the strongest activity (40.63%, 16.84 μmol·L^{-1}) among **TM1** and **TM2** series. This observation indicates that there is a probable relationship between the H-bond acceptors, H-bond donors, and PPARγ activated activity. It is worth noting that the **M5** intermediate has the lowest number of H-bond acceptors (3) and donors (2), but its activity (105.04 %, 25.59 μmol·L^{-1}) is stronger than that of **TM2a**. Similarly, the number of H-bond acceptors and donors of pioglitazone, are all less than those of **TM2a**, but the activity of pioglitazone is stronger than that of **TM2a** and **M5**. Therefore, we thought that the number of H-bonds alone is not the only factor that affected the activity of these molecules.

Table 6

Physical properties of **TM1** and **TM2**.

Compound	cLogP	tPSA	RO5	H-bond acceptors	H-bond donors	Fraction of sp3 carbons	Rotatable bonds	Leadlikeness
Pioglitazone	3.53	67.76	1	4	1	0.32	7	1
M5	2.47	93.73	1	3	2	0.21	9	1
TM1a	1.80	173.52	0	7	4	0.17	13	0
TM1b	2.00	131.11	0	5	2	0.15	10	0
TM1c	2.08	109.33	1	4	2	0.15	10	0
TM1d	3.00	126.51	0	5	2	0.43	12	0
TM1e	2.97	118.12	0	4	3	0.15	11	0
M8	2.23	104.73	1	4	3	0.17	8	1
TM2a	1.50	184.52	0	8	5	0.14	12	0
TM2b	1.70	142.11	1	6	3	0.12	9	0
TM2c	1.78	120.33	1	5	3	0.12	9	0
TM2d	0.43	137.51	0	6	3	**0.41**	11	0
TM2e	2.67	129.12	1	5	4	0.12	10	0

Lipinski's RO5 (drug-likeness) requires mass ≤ 500, cLogP (pH 7.4) ≤ 5, H-bond donors ≤ 5, and H-bond acceptors ≤ 10. Lead-likeness requires mass, 200–350 (optimization might add approximately 100–200); cLogP < 1.0–3.0 (optimization might increase this by 1–2 log units), single charge present (secondary or tertiary amine preferred); and non-substrate

peptides are suitable.

After Lipinski proposed the RO5, other scientists developed more drug-likeness parameters. For example, Fsp^3 is the ratio of the sp^3 hybrid carbon number to total carbon number, which describes the unsaturation of the compound [46]. Studies have shown that a high Fsp3 value indicates that a molecule has more rotatable bonds, which means that its molecular flexibility is better and space adaptability is stronger than that of compounds with low values. A rotatable bond is a single bond other than the single bonds in the ring and C-N bonds [47]. The number of rotatable bonds determines the rigidity and flexibility of a compound. For **TM1** and **TM2**, the number of rotatable bonds is between 8 and 13, more than pioglitazone, indicating that the flexibility of these molecules is better than that of pioglitazone. The Fsp3 values of **TM1d** and **TM2d** were closest to that of pioglitazone, but their PPRE activities are very weak. In contrast, the Fsp3 value of **M5** differs considerably from that of pioglitazone, but its PPRE relative activity is the highest. These data revealed that the molecular activity was not necessarily related to the Fsp3 value, but the appropriate Fsp3 value may help increase molecular flexibility and thus help molecule adapt to protein cavity.

Diabetes is a chronic disease that requires long-term drug administration and, therefore, antidiabetic drugs must have little or no toxicity. To predict the safety of **TM1** and **TM2**, we calculated the toxicity of these compounds using the ADMET Predictor 7.0 software from Simulations Plus, Inc. (USA) (Table 7).

Table 7
Toxicity data of **TM1** and **TM2**.

Compound	hERG pIC50	TOX-RAT (mg/kg)	TOX-BRM-Rat (mg/kg/day)	TOX-BRM-Mouse (mg/kg/day)	TOX-SGPT	TOX-MUT-Risk	TOX-Risk
Pioglitazone	5.16	629.57	4.81	61.68	0	0	1
M5	**5.08**	**672.24**	4.13	**724.74**	0	0	2
TM1a	**5.15**	518.80	3.14	**681.47**	0	0	2
TM1b	5.26	**687.22**	1.69	**829.91**	0	0	2
TM1c	5.31	**844.75**	1.89	**324.03**	0	0	2
TM1d	5.27	278.95	1.89	**686.26**	0	1	3
TM1e	5.23	441.57	1.00	**163.59**	0	0	2
M8	**5.10**	**829.66**	**15.05**	**979.71**	0	0	1
TM2a	**5.16**	**1133.07**	**8.84**	**984.36**	0	0	**0**
TM2b	5.28	**966.63**	**5.95**	**1146.36**	0	0	2
TM2c	5.25	**1253.13**	**5.57**	**519.32**	0	0	1
TM2d	**5.16**	591.56	**6.85**	**999.17**	0	0	**0**
TM2e	**5.12**	391.72	2.98	**265.37**	0	0	1

The human ether-à-go-go-related gene (hERG) is used to quantitatively predict the cardiac toxicity of a compound, and a-log half-maximal inhibitory concentration (pIC50) ≤ 6 $mol \cdot L^{-1}$ is stipulated to be normal. Table 7 shows that the overall performance of the predicted compounds in the order of cardiac toxicity was pioglitazone ≤ **TM2** < **TM1,** the molecules with the lowest predicted cardiac toxicity were **M5**, **M8** and **TM2e**. Totally, the pIC50 values of all predicted molecules were < 6 $mol \cdot L^{-1}$, indicating that they may have no cardiotoxicity.

TOX-RAT predicts the acute toxicity of compounds and is expressed as the median lethal dose (LD_{50}) in rat models. The LD_{50} predictive value of most drug molecules should be ≥ 300 mg/kg. According to Table 7, the predicted acute toxicities of the **TM2** series of molecules, which are more hydrophilic, were lower than that of the **TM1** series.

Furthermore, the predicted acute toxicities of the intermediates **M5** and **M8** were lower than that of pioglitazone. Although the predicted acute toxicities of **TM1d** and **TM2d** (contain Boc piperazine groups), **TM1e** and **TM2e** (contain 2-mercapto benzimidazole groups) were stronger than that of pioglitazone, except for **TM1d**, the LD_{50} of all the molecules were higher than 300 mg/kg and, therefore, they probably lacked acute toxicity.

TOX-BRM-Rat and TOX-BRM-Mouse predict the carcinogenicity of compounds. For most of the drug molecules, the median predictive value of the carcinogenic dose (TD_{50}) should be ≥ 4 and ≥ 25 $mg \cdot kg^{-1} \cdot day^{-1}$ (rat and mouse models, respectively). In the prediction of carcinogenicity in rat, the order of magnitude of carcinogenicity of the compounds was **M8** < **TM2** < pioglitazone < **M5** < **TM1,** and **TM2a** < **TM2d** < **TM2b** < **TM2c** < **TM2e** (8.84, 6.85, 5.95, 5.57, 2.98 $mg \cdot kg^{-1} \cdot day^{-1}$, respectively), where **TM1a** and **TM2a** had the lowest predicted carcinogenicity among that series of compounds. Unfortunately, the **TM1** series and **TM2e** had carcinogenic risk. The predicted results of carcinogenicity in mice revealed the following order **TM2** < **M8** < **M5** < **TM1** < pioglitazone, where **TM2b** < **TM2d** < **TM2a** < **TM2c** < **TM2e** (1146.36, 999.17, 984.36, 519.32, 265.37 $mg \cdot kg^{-1} \cdot day^{-1}$, respectively)，**TM1b** < **TM1d** < **TM1a** < **TM1c** < **TM1e** (829.91, 686.26, 681.47, 324.03, 163.59 $mg \cdot kg^{-1} \cdot day^{-1}$, respectively). **TM1b** and **TM2b** exhibited the lowest predicted carcinogenicity in their respective series, and the order was also consistent in both series. The predicted carcinogenicity of these compounds generally followed the order **TM2** < **TM1** in both the rat or mouse models.

2.3.2 Lead-likeness and toxicity prediction of TM3 and TM4 series

Similarly, we also carried out the physicochemical parameter calculation and toxicity prediction of the **TM3** and **TM4** series (Fig.1). Although **TM3** and **TM4** are parallel structures based on **M5**, due to the different transformation of functional groups, the correlation between the two series of data is very poor. First, the cLogP values of the **TM3** and **TM4** series (0.3–3 and -0.7–4.5, respectively) appeared to meet the RO5 requirements, but the calculated values of most molecules were lower than that of pioglitazone. The tPSA values of the **TM3** and **TM4** series of compounds were in the range of 90–140 and met the requirements for a lead compound, but were higher than that of pioglitazone. The number of rotatable bonds of compound in these two series was between 8 and 12, higher than that of pioglitazone, which indicated that these molecules were more flexible than pioglitazone. The PPARγ activated activity of **TM4a** was only inferior to that of **TM4h**, but its Fsp3 value was the lowest in the **TM4** series. There were five compounds with a similar Fsp3 value to that of pioglitazone, but only **TM4h** showed excellent activity.

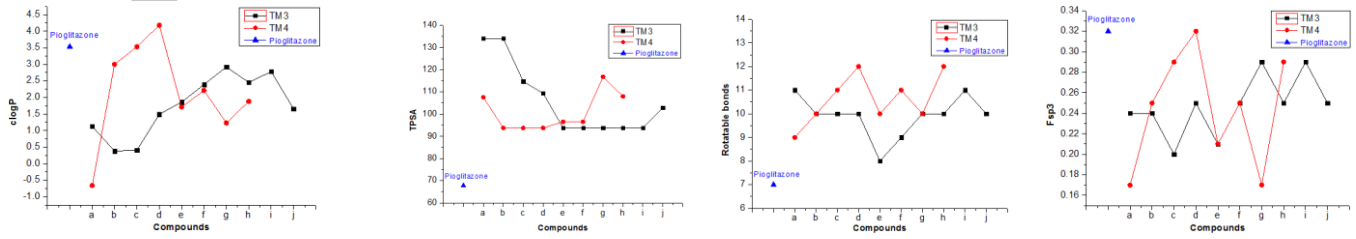

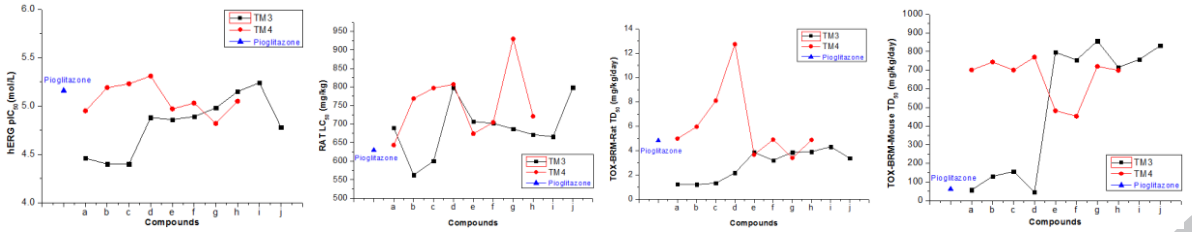

Fig.1. Comparisons of physicochemical properties and toxicities between **TM3** and **TM4** (physicochemical properties in the first row: cLogP, tPSA, Fsp3, and rotatable bonds; predicted toxicity in the second row: hERG, acute toxicity, carcinogenicity in rat and mouse).

Toxicity is an important consideration during the development of new diabetes drugs. The predicted results shown in Fig.1 that the pIC_{50} values of all molecules in the **TM3** and **TM4** series are less than 6 $mol \cdot L^{-1}$, which indicates that they may not have cardiac toxicity.

The predicted results in Fig.1 revealed that all the other molecules in the **TM3** and **TM4** series may have lower acute toxicity levels than that of pioglitazone, except for **TM3b** and **TM3c**. The predicted LD_{50} of all molecules in the **TM3** and **TM4** series was > 300 mg/kg, showing that these compounds may possess no acute toxicity.

The carcinogenicity of the **TM3** and **TM4** molecules was predicted using rat (TOX-BRM-Rat) and mouse (TOX-BRM-Mouse) models and the predicted carcinogenic risk was in the order of **TM4** < **TM3**. All the molecules in the **TM3** and **TM4** series had a lower predicted carcinogenic risk in mice than pioglitazone did, except for **TM3a** and **TM3d**. Therefore, both the **TM3** and **TM4** series showed no predicted carcinogenic risk to mice.

3. Conclusion

We used L-phenylglycine as the starting raw material to prepare novel compounds of the **TM1** and **TM2** series by nitration, α-amino protection, carboxyl protection, nitro reduction, acylation of the amino group on the benzene ring, and reaction with different heterocyclic amines or thiophenol. The assays of PPAR activated activitiy, α-glucosidase inhibitory activity and DPP-4 inhibitory activity identified one novel compound (**M5**) with high PPRE relative activity. We adapted **M5** as a hit compound and subsequently designed and synthesized the **TM3** and **TM4** series of molecules by replacing the chlorine atom or methyl ester of **M5** with other moieties. The results of the PPRE relative activity assay revealed that **TM4h** had the highest PPRE relative activity. The calculation of physicochemical properties and prediction of toxicities suggested that **TM4h** is worth further investigation. Finally, this study established the structure-activity relationship of the target molecules, which has provided ideas and directions for further research studies.

4. Experimental section

4.1 Reagents and instrumentation

Melting points were determined by an electrothermal X-6 apparatus. ^{1}H NMR and ^{13}C NMR spectra were recorded on a Bruker AV 300 spectrometer using TMS as an internal standard. The chemical shifts were reported in parts per million (ppm), the coupling constants (J) are expressed in hertz (Hz) and signals were described as singlet (s), doublet (d), triplet (t), quartet (q), as well as multiplet (m). ESI-MS analyses were obtained on an Agilent 1946B instrument. High resolution mass spectra (HRMS) analyses were conducted on a Daltonics Data Analysis 3.2 (Bruker) using ESI (electrospray ionization) techniques. The purity of the compounds was examined by thin-layer

chromatography (TLC) on silica gel plate using petroleum ether and ethyl acetate. All chemical reagents and solvents were commercially available, and were used without further purification [16].

4.2 Chemistry

4.2.1 Preparation of M1 and M2

M1 and **M2** have been reported by our laboratory [26, 27].

4.2.2 Preparation of M3

In a round bottom bottle，$SOCl_2$ (2.2 mmol) was added dropwise into methanol (10 mL) at ice-water temperature. After stirring 0.5 h, **M2** (2.1 mmol) was added into the mixture solution. The resultant mixture was refluxed at 70℃and monitored by TLC. The crude product was obtained through concentrating under reduced pressure. Added a small amount of methanol to dissolve the residue, dropped cooled petroleum ether to precipitate the target compound. After a large amount of white solid appeared, filtrated, washed with water three times, and dried *in vacuo*, the pure **M3** was obtained.

M3: Benzyl (S)-(methoxycarbonyl)(3-nitrophenyl)methylcarbamate

Yield 83%, m.p.: 93~94℃. **^{1}H NMR** (DMSO-d_6, 300 MHz) ***δ:*** 3.76(s, 3H, -$COOCH_3$)， 5.04~5.15(m, 2H, $ArCH_2O$), 5.49(d, *J*=6.4 Hz, 1H, CH), 6.11(d, *J*=5.36 Hz, 1H, -CONH-), 7.26~7.35(m, 4H, ArH), 7.56(t, 1H, J_1=7.9 Hz, J_2=7.8 Hz, ArH), 7.75 (d, *J*=7.4 Hz, 1H, ArH), 8.18~8.26(m, 2H, ArH); **^{13}C NMR** (DMSO-d_6, 75 MHz) ***δ***: 53.3, 57.2, 67.4, 122.0, 123.5, 128.2, 128.3, 128.5, 129.8, 133.3, 135.7, 139.0, 148.5, 155.2, 169.9.

4.2.3 Preparation of M4

The mixture of **M3** (1.1 mmol), Zn powder (11.8 mmol), ammonium chloride (6.4 mmol) and ethyl acetate (EtOAc, 10 mL) in a 50 mL round bottom flask was stirred at 75 ℃and monitored by TLC until completion. After hot filtration, the EtOAc was employed to wash the residue on the filter paper to ensure that products obtained were all dissolved in the filtrate. The combined filtrate was washed with water (3×6 mL), and dried over anhydrous Na_2SO_4. The organic solvent was then removed under reduced pressure, and thus the yellow crude product **M4** was obtained. Without further purification, the crude product was used directly in the synthesis of **M5**.

4.2.4 Preparation of M5

M4 (12.1 mmol), dried acetone (10 mL), anhydrous K_2CO_3 (36.4 mmol) were added into the 50 mL round bottom flask. While the resultant mixture was stirred in an ice bath, the acetone solution (10 mL) of chloroacetyl chloride (12.7 mmol) was dripped slowly from the constant pressure funnel. After 5 min, removed the ice bath, stirred the reaction solution at 10℃and monitored the reaction process by TLC. Upon completion, filtrated off potassium carbonate, distilled under reduced pressure, added EtOAc (25 mL) and saturated brine (10 mL), extracted with EtOAc (3×12 mL), dried over anhydrous Na_2SO_4, concentrated to remove the solvent, and the crude product **M5** was obtained. The crude products were recrystallized from choroform/petroleum ether to give a white solid, that is the pure product **M5**.

M5: Methyl (S)-2-(benzyloxycarbonylamino)-2-(3-(2-chloroacetamido)phenyl)acetate

Yield 80%, m.p.: 170~171℃, $[\alpha]_D^{20}$ +22.0(c 1.0 mg/mL, Acetone). **^{1}H NMR** (DMSO-d_6, 300 MHz) ***δ:*** 3.64(s,

3H, -$COOCH_3$)，4.25(s, 2H, $COCH_2Cl$), 5.06(s, 2H, $ArCH_2O$), 5.25(d, *J*=7.5 Hz, 1H, CH), 7.12(d, *J*=7.6 Hz, 1H, ArH), 7.30~7.36(m, 6H, ArH), 7.60(d, *J*=12.9 Hz, 2H, ArH), 8.32(d, *J*=7.4 Hz, 1H, -CONH-), 10.40(s, 1H, -CONH-). **^{13}C NMR** (DMSO-d_6, 75 MHz) ***δ:*** 43.6, 52.3, 58.0, 65.8, 118.8, 119.3, 123.3, 127.8, 127.9, 128.4, 129.2, 136.9, 137.0, 138.7, 155.9, 164.8, 171.1; **HR ESI-MS** calcd for $C_{19}H_{19}ClN_2O_5$ $[M-H]^-$ 389.0910，found 389.0915.

4.2.5 General preparation of TM1

In a 50 mL flask, Y^1-H (1.1 mmol), dimethyl formamide (2.0 mL) and fine anhydrous potassium carbonate (1.3 mmol) were added. After stirring vigorously 0.5 hour, added the compound **M5** (0.9 mmol). Stirred evenly at room temperature, and monitored the reaction process by TLC. After completion, added saturated brine (15 mL) to the reaction mixture, adjusted pH to 5 ~ 6 with 2 mol/L hydrochloric acid in an ice bath, extracted by EtOAc (3 × 10 ml), combined the organic layer, washed with saturated brine (15 mL), dried over anhydrous Na_2SO_4, the crude product was obtained by drying *in vacuo*, and the pure **TM1** was obtained furtherly by silica gel column chromatography or recrystallization.

TM1a：Methyl (S)-2-(((benzyloxy)carbonyl)amino)-2-(3-(2-((4-(*N*-(5-methylisoxazol-3-yl)sulfamoyl) phenyl)amino)acetamido)phenyl)acetate

Yield 38%, m.p.: 195~197℃, $[\alpha]_D^{20}$ +19.0(c 1.0 mg/mL, Acetone). **^{1}H NMR** (DMSO-d_6, 300 MHz) ***δ:*** 2.3(s, 3H, CH_3)，3.63(s, 3H, -$COOCH_3$)，4.49(s, 2H, $COCH_2$), 5.06(s, 2H, $ArCH_2O$), 5.22(d, *J*=7.1 Hz, 1H, CH), 6.25(S, 1H, NH), 6.40(s, 1H, -C=CH-), 6.62(d, *J*=7.9 Hz, 2H, ArH), 7.08(d, *J*=7.4 Hz, 1H, ArH), 7.30~7.36(m, 6H, ArH), 7.51~7.56(m, 4H, ArH), 7.94(s, 1H, -CONH-) 8.21(d, *J*=7.2 Hz, 1H, -CONH-), 10.24(s, 1H, -SO_2NH-); **^{13}C NMR** (DMSO-d_6, 75 MHz) ***δ:*** 12.1, 50.2, 52.3, 59.8, 65.7, 96.7, 112.8, 118.4, 118.8, 122.0, 122.8, 128.4, 129.1, 129.4, 136.8, 139.0, 154.0, 155.9, 159.5, 162.3, 165.2, 170.4, 171.1; **HR ESI-MS** calcd for $C_{29}H_{29}N_5O_8S$ $[M+Na]^+$630.1624，found 630.1625.

TM1b: Methyl (S)-2-(benzyloxycarbonylamino)-2-(3-(2-(1,3-dioxoisoindolin-2-yl)acetamido)phenyl) acetate

Yield 75%, m.p.: 98~100℃, $[\alpha]_D^{20}$ +46.0(c 1.0 mg/mL, Acetone); $[\alpha]_D^{20}$ +25.0(c 1.0 mg/mL, EtOAc). **^{1}H NMR** (DMSO-d_6, 300 MHz) ***δ:*** 3.64(s, 3H, -$COOCH_3$), 4.01(s, 2H, $COCH_2$)，5.07(s, 2H, $ArCH_2O$), 5.25(d, *J*=7.3 Hz, 1H, CH), 7.15(d, *J*=7.3 Hz, 1H, ArH), 7.32~7.95(m, 12H, ArH), 8.33(d, *J*=7.4 Hz, 1H, -CONH-), 9.89(s, 1H, -CONH-). **^{13}C NMR** (DMSO-d_6, 75 MHz) ***δ:*** 43.4, 52.3, 58.1, 65.7, 118.9, 119.2, 122.7, 127.7, 128.4, 129.0, 129.4, 130.0, 131.7, 136.8, 138.2, 138.9, 155.9, 168.0, 169.1, 171.1; **HR ESI-MS** calcd for $C_{27}H_{23}N_3O_7$[M-H]$^-$ 500.1463，found 500.1455.

TM1c: Methyl (S)-2-(3-(2-(*1H*-benzo[d]imidazol-1-yl)acetamido)phenyl)-2-(benzyloxycarbonylamino) acetate

Yield 66%, m.p.: 114~115℃, $[\alpha]_D^{20}$ +17.0(c 1.0 mg/mL, EtOAc). **^{1}H NMR** (DMSO-d_6, 300 MHz) ***δ:*** 3.62(s, 3H, -$COOCH_3$)，5.05(s, 2H, $ArCH_2O$), 5.20(s, 2H, $COCH_2$), 5.24(d, *J*=7.1 Hz, 1H, CH), 7.11(d, *J*=7.4 Hz, 1H, ArH), 7.19~7.35(m, 7H, ArH), 7.52~7.69(m, 5H, ArH), 8.24(s, 1H, -N=CH-), 8.31(d, *J*=6.9 Hz, 1H, -CONH-), 10.57(s, 1H, -CONH-); **^{13}C NMR** (DMSO-d_6, 75 MHz) ***δ:*** 30.7, 52.3, 58.0, 65.7, 110.3, 119.3, 122.4, 123.1, 127.8, 128.4, 129.2, 134.4, 136.8, 137.1,138.8, 143.2, 145.0, 155.9, 165.6, 171.0. **HR ESI-MS** calcd for $C_{26}H_{26}N_4O_5$[M-H]$^-$ 473.1825，found 473.1824.

TM1d: Tert-butyl (S)-4-(2-(3-(1-(benzyloxycarbonylamino)-2-methoxy-2-oxoethyl)phenylamino)-2- oxoethyl)

piperazine-1-carboxylate

Yield 73%, m.p.: 101~102℃, $[\alpha]_D^{20}$ +37.0(c 1.0 mg/mL, EtOAc). **^{1}H NMR** ($CDCl_3$, 300 MHz) ***δ:*** 1.48(s, 9H, $C(CH_3)_3$), 2.57(s, 4H, CH_2 and CH_2), 3.15(s, 2H, $COCH_2$)，3.52(s, 4H, CH_2 and CH_2), 3.73(s, 3H, -$COOCH_3$), 5.04~5.15(m, 2H, $ArCH_2O$), 5.35(d, J=6.7 Hz, 1H, CH), 5.90(d, *J*=6.3 Hz, 1H, -CONH-), 7.12(d, *J*=7.1 Hz, 1H, ArH), 7.26(s, 1H, ArH), 7.35(s, 5H, ArH), 7.46(s, 1H, ArH), 7.69(d, *J*=7.4 Hz, 1H, ArH), 9.05(s, 1H, -CONH-); **^{13}C NMR** ($CDCl_3$, 75 MHz) ***δ:*** 28.3, 43.4, 52.9, 53.2, 57.8, 62.1, 67.1, 80.0, 118.1, 119.8, 122.9, 128.2, 128.5, 129.7, 136.0, 137.6, 137.9, 154.6, 155.3, 168.0, 171.0; **HR ESI-MS** calcd for $C_{28}H_{36}N_4O_7[M-H]^-$ 539.2511，found 539.2511.

TM1e: Methyl (S)-2-(3-(2-(*1H*-benzo[d]imidazol-2-ylthio)acetamido)phenyl)-2-(benzyloxycarbonyl -amino)acetate

Yield 85%, m.p.: 95~96℃, $[\alpha]_D^{20}$ +17.0(c 1.0 mg/mL, EtOAc). **^{1}H NMR** ($CDCl_3$, 300 MHz) ***δ:*** 3.65(s, 3H, -$COOCH_3$), 3.92(s, 2H, $COCH_2$)，5.01~5.13(m, 2H, $ArCH_2O$), 5.33(d, *J*=6.9 Hz, 1H, CH), 5.94(d, *J*=6.9 Hz, 1H, -CONH-), 7.07(d, *J*=7.4 Hz, 1H, ArH), 7.22~7.31(m, 9H, ArH), 7.51(d, *J*=6.0 Hz, 3H, ArH, NH), 7.63(s, 1H, -CONH-); **^{13}C NMR** ($CDCl_3$, 75 MHz) ***δ:*** 36.1, 52.9, 57.8, 67.2, 118.3, 119.8, 122.7, 128.0, 128.5, 129.6, 135.9, 137.2, 138.9, 150.5, 155.5, 168.2, 171.0. **HR ESI-MS** calcd for $C_{26}H_{24}N_4O_5S[M-H]^-$ 503.1395，found 503.1401.

4.2.6 General preparation of TM2

TM1 (0.4 mmol), THF (2.0 mL) were added into the 50 mL flask. While stirring and cooling in an ice bath, added 1 mol/L LiOH solution to adjust pH to 10~11. Stirred the mixture at room temperature, and monitored by TLC until completion. After adding saturated brine (10 mL), adjusted pH to 5~6 with 2 mol/L hydrochloric acid. Extracted with EtOAc (3×8 mL), combined the organic layer, dried over anhydrous Na_2SO_4, then the filtrate was concentrated under reduced pressure to give pure **TM2.**

TM2a : (S)-2-(((benzyloxy)carbonyl)amino)-2-(3-(2-((4-(*N*-(5-methylisoxazol-3-yl)sulfamoyl)phenyl) amino)acetamido)phenyl)acetic acid

Yield 86%, m.p.: 235~236℃, $[\alpha]_D^{20}$ +19.7(c 1.0 mg/mL, DMF). **^{1}H NMR** (DMSO-d_6, 300 MHz) ***δ:*** 2.3(s, 3H, CH_3), 4.49(s, 2H, $COCH_2$), 5.06(s, 2H, $ArCH_2O$), 5.22(d, *J*=7.1 Hz, 1H, CH), 6.25(S, 1H, NH), 6.40(s, 1H, CH), 6.62(d, *J*=7.9, Hz 2H, ArH), 7.08(d, *J*=7.4 Hz, 1H, ArH), 7.30~7.36(m, 6H, ArH), 7.51~7.56(m, 4H, ArH), 7.94(s, 1H, -CONH-) 8.21(d, *J*=7.2 Hz, 1H, -CONH-), 10.24(s, 1H, -SO_2NH-); **^{13}C NMR** (DMSO-d_6, 75 MHz) ***δ:*** 12.4, 50.2, 59.8, 65.7, 96.7, 112.8, 118.4, 118.8, 122.0, 122.8, 128.4, 129.1, 129.4, 136.8, 139.0, 154.0, 155.9, 159.5, 162.3, 165.2, 170.4, 171.1; **HR ESI-MS** calcd for $C_{28}H_{27}N_5O_8S$ $[M+Na]^+$616.1467，found 616.1467.

TM2b: (S)-2-(((benzyloxy)carbonyl)amino)-2-(3-(2-(1,3-dioxoisoindolin-2-yl)acetamido)phenyl)acetic acid

Yield 83%, m.p.: 177~178℃, $[\alpha]_D^{20}$ +29.7(c 1.0 mg/mL, DMF). **^{1}H NMR** (DMSO-d_6, 300 MHz) ***δ:*** 4.01(s, 2H, $COCH_2$)，5.07(s, 2H, $ArCH_2O$), 5.25(d, *J*=7.3 Hz, 1H, CH), 7.15(d, *J*=7.3 Hz, 1H, ArH), 7.32~7.95(m, 12H, ArH), 8.33(d, *J*=7.4 Hz, 1H, -CONH-), 9.89(s, 1H, -CONH-). **^{13}C NMR** (DMSO-d_6, 75 MHz) ***δ:*** 43.4, 58.1, 65.7, 118.9, 119.2, 122.7, 127.7, 128.4, 129.0, 129.4, 130.0, 131.7, 136.8, 138.2, 138.9, 155.9, 168.0, 169.1, 171.1; **HR ESI-MS**

calcd for $C_{26}H_{21}N_3O_7$[M-H]$^-$ 486.1301，found 486.1302.

TM2c: (S)-2-(3-(2-(1*H*-benzo[d]imidazol-1-yl)acetamido)phenyl)-2-(((benzyloxy)carbonyl)amino) acetic acid

Yield 87%, m.p.: 169~171℃, $[\alpha]_D^{20}$ +19.9(c 1.0 mg/mL, DMF). **^{1}H NMR** (DMSO-d_6, 300 MHz) ***δ:*** 3.99(s, 2H, $COCH_2$), 5.05(s, 2H, $ArCH_2O$), 5.13(d, 2H, $COCH_2$), 5.24(d, *J*=7.1 Hz, 1H, CH) 7.11(d, *J*=7.8 Hz, 1H, ArH), 7.31~7.85(m, 12H, ArH), 8.10(d, *J*= 7.8 Hz, 1H, -OCONH-), 8.76(d, *J*=5.7 Hz, 1H, -N=CH-), 9.86(s, 1H, -CONH-). **^{13}C NMR** (DMSO-d_6, 75 MHz) ***δ:*** 30.7, 58.0, 65.7, 110.3, 119.3, 122.4, 123.1, 127.8, 128.4, 129.2, 134.4, 136.8, 137.1,138.8, 143.2, 145.0, 155.9, 165.6, 171.0. **HR ESI-MS** calcd for $C_{25}H_{24}N_4O_5$[M-H]$^-$ 459.1668，found 459.1669.

TM2d: (S)-2-(((benzyloxy)carbonyl)amino)-2-(3-(2-(4-(tert-butoxycarbonyl)piperazin-1-yl)acetamido) phenyl)acetic acid

Yield 95%, m.p.: 151~153℃, $[\alpha]_D^{20}$ +45.0(c 1.0 mg/mL, DMF). **^{1}H NMR** (DMSO-d_6, 300 MHz) ***δ:*** 1.42(s, 9H, $-C(CH_3)$), 2.04~2.09(m, 4H, $2CH_2$), 3.02~3.23(m, 4H, $2CH_2$), 4.02(s, 2H, $-COCH_2$), 5.05(s, 2H, $ArCH_2O$), 5.13(d, *J*= 7.8 Hz, 1H, CH), 7.16(d, *J*= 7.2 Hz, 1H, ArH), 7.31~7.36(m, 6H, ArH), 7.59~7.64(m, 2H, ArH), 8.14(d, *J*= 7.8 Hz, 1H, -OCONH-), 10.48(s, 1H, -CONH-); **^{13}C NMR** (DMSO-d_6, 75 MHz) ***δ:*** 28.4, 31.1, 52.0, 57.8, 58.5, 66.0, 80.2, 119.4, 119.5, 123.6, 128.1, 128.2, 128.8, 129.4, 137.2, 138.3, 138.5, 153.9, 156.2, 172.3; **HR ESI-MS** calcd for $C_{27}H_{34}N_4O_7$ $[M+Na]^+$ 549.2320, found 549.2327.

TM2e: (S)-2-(3-(2-((1*H*-benzo[d]imidazol-2-yl)thio)acetamido)phenyl)-2-(((benzyloxy)carbonyl) amin o)acetic acid

Yield 90%, m.p.: 147~149℃, $[\alpha]_D^{20}$ +24.0(c 1.0 mg/mL, DMF). **^{1}H NMR** (DMSO-d_6, 300 MHz) ***δ:*** 4.60(s, 2H, $COCH_2$), 5.04(s, 2H, $ArCH_2O$), 5.09~5.18(m, 2H, CH and -NHC=N-), 7.12(d, 1H, *J*= 7.5 Hz, ArH), 7.27~7.35(m, 8H, ArH), 7.42~7.65(m, 4H, ArH), 8.13(d, 1H, *J*= 7.8 Hz, -OCONH-), 10.46(s, 1H, -CONH-); **^{13}C NMR** ($CDCl_3$, 75 MHz) ***δ:*** 36.1, 57.8, 67.2, 118.3, 119.8, 122.7, 128.0, 128.5, 129.6, 135.9, 137.2, 138.9, 150.5, 155.5, 168.2, 171.0. **HR ESI-MS** calcd for $C_{25}H_{22}N_4O_5S$ [M-H]$^-$ 489.1233，found 489.1238.

4.2.7 General preparation of TM3

The synthetic conditions of **TM3a~TM3d** from **M5** are the same as **TM1**.

The preparative procedure of **TM3e~TM3j** from **M4**. **M4** (0.314 g, 1.0 mmol), acetone (4 ml) and anhydrous K_2CO_3 (0.414 g, 3.0 mmol) were added to the 50 mL round bottom flask, cooled in an ice bath, and the RCH_2COCl (2.0 mmol) was added dropwise. Then the reaction mixture was stirred at 20~30℃ and detected by TLC. Upon completion, the saturated brine was added, the pH of the solution was adjusted to 5 - 6 with 2 mol/L HCl in ice bath. After the acetone was removed, the residue was extracted by EtOAc (3×10 mL). The combined organic phase was washed with saturated brine (3×10 mL), dried over anhydrous Na_2SO_4, then the crude product was obtained by vacuum distillation, and the purified **TM3e - TM3j** was obtained by silica gel column chromatography.

TM3a: Methyl (S)-2-(benzyloxycarbonylamino)-2-(3-(2-(5-(methylthio)-1*H*-tetrazol-1-yl)acetamido) phenyl)acetate

Yield 66%, m.p.: 182~183℃, $[\alpha]_D^{20}$ +11.0(*c*=1.0 mg /mL, EtOAc). **^{1}H NMR** ($CDCl_3$, 300 MHz) ***δ:*** 3.74 (s, 3H, -$COOCH_3$), 3.98(s, 3H, SCH_3), 4.06(s, 2H, $ArCH_2O$), 5.15(s, 2H, CH_2CO), 5.35(d, *J*=7.01 Hz, 1H, -CONH-), 5.90(s, 1H, CH), 7.13(d, *J*=7.3 Hz, 2H, ArH), 7.28~7.36(m, 5H, ArH), 7.51(d, *J*=7.8 Hz, 1H, ArH), 7.60(s, 1H, ArH), 9.45(s, 1H, -CONH-); **^{13}C NMR** (DMSO-d_6, 75 MHz) ***δ:*** 31.1, 43.9, 52.7, 58.4, 66.1, 119.2, 119.6, 123,6, 128.2, 128.3, 128.8, 129.6, 137.2, 137.4, 138.9, 156.2, 165.2, 171.4; **HRMS** calcd for $C_{21}H_{22}N_6O_5S[M-H]^-$ 469.1300, found 469.1297.

TM3b: Methyl (S)-2-(benzyloxycarbonylamino)-2-(3-(2-(5-methyl-1*H*-tetrazol-1-yl)acetamido) phenyl) acetate

Yield 55%, m.p.: 156~157℃, $[\alpha]_D^{20}$ +24.0(c 1.0 mg/mL, EtOAc). **^{1}H NMR** (DMSO-d_6, 300 MHz) ***δ:*** 2.57(s, 3H, CH_3), 3.76(s, 3H, -$COOCH_3$)，5.14(s, 4H, $ArCH_2O$ and $COCH_2$), 5.31(d, *J*=6.3 Hz, 1H, CH), 6.18 (d, *J*=6.3 Hz, 1H, -CONH-), 7.12(d, *J*=7.2 Hz, 1H, ArH), 7.20~7.51(m, 7H, ArH), 7.62(s, 1H, ArH), 8.84(s, 1H, -CONH-); **^{13}C NMR** (DMSO-d_6, 75 MHz) ***δ:*** 8.8, 49.8, 53.0, 57.9, 67.2, 118.7, 120.1, 123,4, 127.9, 128.2, 128.5, 129.7, 136.0, 137.6, 137.7, 155.6, 162.7, 170.8; **HRMS** calcd for $C_{21}H_{22}N_6O_5$ $[M+ Na]^+$ 461.1544, found 461.1546.

TM3c: Methyl (S)-2-(3-(2-(1*H*-tetrazol-1-yl)acetamido)phenyl)-2-(((benzyloxy)carbonyl)amino) acetate

Yield 53%, m.p.: 130~131℃, $[\alpha]_D^{20}$ +33.0(c 1.0 mg/mL, Acetone). **^{1}H NMR** (DMSO-d_6, 300 MHz) ***δ:*** 3.63(s, 3H, -$COOCH_3$)，5.06(s, 2H, $ArCH_2O$), 5.24(d, *J*=7.5 Hz, 1H, CH), 5.49(s, 2H, $COCH_2$), 7.13(d, *J*=7.5 Hz, 1H, ArH), 7.31~7.36(m, 6H, ArH), 7.57(d, *J*=9.3 Hz, 2H, ArH), 8.33(d, *J*=7.5 Hz, 1H, -CONH-), 9.43(s, 1H, -N=CH-), 10.65(s, 1H, -CONH-); **^{13}C NMR** (DMSO-d_6, 75 MHz) ***δ:*** 50.5, 52.8, 58.3, 60.2, 66.2, 119.1, 119.5, 123.7, 128.1, 128.2, 128.3, 128.7, 129.7, 137.2, 137.5, 138.8, 145.7, 156.3, 164.0, 171.4; **HRMS** calcd for $C_{20}H_{20}N_6O_5[M-H]^-$ 423.1422, found 423.1426.

TM3d: Methyl (S)-2-(((benzyloxy)carbonyl)amino)-2-(3-(2-(3,5-dimethyl-1*H*-pyrazol-1-yl)acetamido) phenyl)acetate

Yield 32%, m.p.: 135~136℃, $[\alpha]_D^{20}$ +17.0(c 1.0 mg/mL, EtOAc). **^{1}H NMR** (DMSO-d_6, 300 MHz) ***δ:*** 3.62(s, 3H, -$COOCH_3$)，5.05(s, 2H, $ArCH_2O$), 5.20(s, 2H, $COCH_2$), 5.24(d, *J*=7.1 Hz, 1H, CH), 7.11(d, *J*=7.4 Hz, 2H, ArH), 7.19~7.35(m, 7H, ArH), 8.24(s, 1H, CH), 8.31(d, *J*=6.9 Hz, 1H, -CONH-), 10.57(s, 1H, -CONH-); **^{13}C NMR** (DMSO-d_6, 75 MHz) ***δ:*** 30.7, 52.3, 58.0, 65.7, 110.3, 119.3, 122.4, 123.1, 127.8, 128.4, 129.2, 134.4, 136.8, 137.1,138.8, 143.2, 145.0, 155.9, 165.6, 171.0. **HRMS** calcd for $C_{24}H_{26}N_4O_5$ $[M-H]^-$ 449.1825，found 449.1826.

TM3e: Methyl (S)-2-(3-acetamidophenyl)-2-(benzyloxy)carbonyl)amino)acetate

Yield 65%, m.p.: 127~128℃.**^{1}H NMR** (DMSO-d_6, 300 MHz) ***δ:*** 3.03(s, 3H, -$COCH_3$), 3.63(s, 3H, -$COOCH_3$), 5.06(s, 2H, $ArCH_2O$), 5.20(d, *J*=7.5Hz, 1H, CH), 7.05(d, *J*=7.8Hz, 1H, ArH), 7.25~7.36(m, 6H, ArH), 7.57 (t, *J*=8.1Hz, 2H, ArH), 8.29(d, *J*=7.5Hz, 1H, -CONH-), 10.01(s, 1H, -CONH-); **^{13}C NMR** (DMSO-d_6, 75 MHz) ***δ:*** 24.4, 52.7, 58.5, 66.1, 118.9, 119.3, 122.7, 128.2, 128.3, 128.8, 129.4, 137.1, 137.2, 140.0, 156.3, 168.8, 171.5. **HRMS** calcd for $C_{19}H_{20}N_2O_5[M+Na]^+$ 379.1264, found 379.1271.

TM3f: Methyl (S)-2-(((benzyloxy)carbonyl)amino)-2-(3-propionamidophenyl)acetate

Yield 53%, m.p.: 136~137℃, $[\alpha]_D^{20}$ =+26.0°(c=1.0 mg/mL, EtOAc). **^{1}H NMR** ($CDCl_3$, 300 MHz) δ: 1.25(t, J = 4.2 Hz, 3H, CH_2**CH3**), 2.35-2.43(m, 2H, **CH_2**CH_3), 3.79(s, 3H, CH_3), 5.09(s, 2H, $ArCH_2O$), 5.33(d, J = 4.2 Hz, 1H, CH), 7.29(s, 1H, ArH) 7.35(s, 5H, ArH), 7.46-7.52 (m, 2H, ArH), 7.85(d, J = 7.2 Hz, 1H, ArH). **^{13}C NMR** ($CDCl_3$, 75 MHz) δ: 29.7, 52.9, 57.9, 67.1, 118.4, 120.0, 122.6, 127.8, 128.2, 128.5, 129.6, 135.9, 137.3, 138.7, 155.4, 171.1, 172.3. **HRMS** calcd for $C_{20}H_{22}N_2O_5$[M+Na] $^+$393.1421, found 393.1427.

TM3g: Methyl (S)-2-(((benzyloxy)carbonyl)amino)-2-(3-butyramidophenyl)acetate

Yield 51%, m.p.: 140~141℃, $[\alpha]_D^{20}$ =+33.0°(c=1.0 mg/mL, EtOAc). **^{1}H NMR** (DMSO-d_6, 300 MHz) δ: 0.90(t, J = 7.2 Hz, 3H, CH_2**CH_3**), 1.55-1.63(m, 2H, **CH_2**CH_3), 2.26(t, J = 7.2 Hz, 2H, -CH_2**CH_2**CO-), 3.62(s, 3H, OCH_3), 5.05(s, 2H, $ArCH_2O$), 5.19(d, J=7.2 Hz, 1H, CH), 7.04(d, J = 7.5 Hz, 1H, ArH) 7.35(m, 6H, ArH), 7.57(m, 2H, ArH), 8.26(d, J = 7.5 Hz, 1H, CONH), 9.94(s, 1H, CONH). **^{13}C NMR** (DMSO-d6, 75 MHz) δ: 14.1, 19.0, 38.7, 52.7, 58.5, 66.1, 119.3, 122.7, 128.2, 128.3, 128.8, 129.4, 137.1, 137.2, 139.9, 156.4, 171.5, 171.7, 118.9. **HRMS** calcd for $C_{21}H_{24}N_2O_5$ $[M+Na]^+$407.1577, found 407.1574.

TM3h: Methyl (S)- 2-(((benzyloxy)carbonyl)amino)-2-(3-(3-chlorobutanamido)-phenyl)acetate

Yield 65%, m.p.: 152~154℃, $[\alpha]_D^{20}$ =+22.0°(c=1.0 mg/mL, EtOAc). **^{1}H NMR** ($CDCl_3$, 300 MHz) δ: ($CDCl_3$, 300 MHz) δ: 2.78(t, J = 6.3 Hz, 2H, -$COCH_2$), 3.71(s, 3H, -OCH_3), 3.86(t, J = 6.3 Hz, 2H, -CH_2Cl), 5.09(d, J = 4.2Hz, 2H, $ArCH_2O$), 5.33(d, J=6.9 Hz, 1H, CH), 7.10(d, J = 7.8 Hz, 1H, ArH), 7.29-7.33(m, 5H, ArH), 7.48(s,1H, ArH), 7.55(d, J = 7.5 Hz, 1H, ArH), 7.70(s, 1H, ArH). **^{13}C NMR** ($CDCl_3$, 75 MHz) δ: 39.8, 40.2, 52.9, 57.9, 67.2, 118.7, 120.2, 122.9, 128.1, 128.2, 128.5, 129.6, 135.9, 137.3, 138.4, 155.5, 168.2, 171.1. **HRMS** calcd for $C_{20}H_{21}ClN_2O_5$ $[M+Na]^+$ 427.1035, found 427.1031

TM3i: Methyl (S)-2-(((benzyloxy)carbonyl)amino)-2-(3-(4-chloropropanamido)phenyl)acetate

Yield 62%, m.p.: 158~160℃, $[\alpha]_D^{20}$ =+59.0°(c=1.0 mg/mL, EtOAc). **^{1}H NMR** δ: 2.17-2.24(m, 2H, -CH_2**CH_2**CH_2-), 2.52(t, J = 7.8 Hz, 2H, -$COCH_2$), 2.67(t, J = 5.4 Hz, 2H, -CH_2Cl), 3.72(s, 3H, OCH_3), 5.08(d, J=3.3 Hz, 2H, $ArCH_2O$), 5.35(d, J = 9.6 Hz, 1H, -CH), 7.09(s, 1H, ArH), 7.29-7.34(m, 6H, ArH), 7.49(s, 1H, ArH), 7.58(m, 1H, ArH). **^{13}C NMR** ($CDCl_3$, 75 MHz) δ: 26.8, 33.2, 42.8, 52.5, 57.6, 66.8, 118.7, 120.3, 122.8, 128.1, 128.2, 128.5, 129.6, 136.0, 137.3, 138.6, 156.2, 171.5, 175.8. **HRMS** calcd for $C_{21}H_{23}ClN_2O_5$ $[M+Na]^+$ 441.1182, found 441.1184.

TM3j: Methyl (S)-2-(((benzyloxy)carbonyl)amino)-2-(3-(2-methoxyacetamido)phenyl)acetate

Yield 52%, m.p.: 116~117℃,**^{1}H NMR** (DMSO-d_6, 300 MHz) ***δ:*** 3.37(s, 3H, -OCH_3), 3.64(s, 3H, -$COOCH_3$), 3.99(s, 2H, $COCH_2O$), 5.06(s, 2H, $ArCH_2O$), 5.23(d, *J*=7.5Hz, 1H, CH), 7.09(d, *J*=7.5Hz, 1H, ArH), 7.27~7.36(m, 5H, ArH), 7.64 (t, J_1=7.5, 3H, ArH), 8.28(d, *J*=7.8, 1H, -CONH-), 9.82(s, 1H, -CONH-). **^{13}C NMR** ($CDCl_3$, 75 MHz) δ: 52.7, 59.1, 66.1, 72.1, 119.7, 119.9, 120.3, 123.3, 128.1, 128.2, 128.3, 128.6, 128.8, 129.3, 131.5, 137.2, 139.0, 156.3, 168.6, 171.5. **HRMS** calcd for $C_{20}H_{22}N_2O_6$[M+Na]$^+$ 409.1365, found 409.1366.

4.2.8 Preparation of M6

Preparation of **M6b~M6d**: $SOCl_2$ (5.3 mmol) was added dropwise into alcohols (15 mL) in an ice salt bath. After stirring for 0.5 h, **M2** (5.0 mmol) was added into the above solution. The resulting mixture was refluxed at 70℃ and monitored by TLC until completion. The crude product was obtained through concentrating under reduced pressure, followed by recrystallization with alcohol and petroleum ether to give white solid **M6b~M6d**.

Preparation of **M6e~ M6h**: To a solution of **M2** (0.5 mmol) and HOBt (0.6 mmol) in dried THF (2 mL) which was cooled to 0℃, dicyclohexylcarbodiimide (DCC, 0.6 mmol) and DIPEA (0.25 mmol) were added. The mixture was stirred in an ice-water bath for 0.5 h and amines (0.6 mmol) was added. The resulting reaction mixture was stirred at room temperature and monitored by TLC until completion. Filtered by suction and washed the filter cake with cold EtOAc (3×3 mL).The combined filtrate was concentrated under reduced pressure, the obtained residue was dissolved by EtOAc (20 mL), and then washed with 0.5*N* $NaHCO_3$ (10 mL×3), 10% citric acid (10 mL×3) and saturated brine (10 mL) sequentially. The organic solution was dried over Na_2SO_4, concentrated *in vacuo*, the residue was purified through silica gel column chromatography to give **M6e~ M6h**.

M6b: Ethyl (S)-2-(benzyloxycarbonylamino)-2-(3-nitrophenyl)acetate

Yield 85%, m.p.: 109~110℃. **^{1}H NMR** (DMSO-d_6, 300 MHz) ***δ:*** 1.12(t, *J*=6.8 Hz, 3H, CH_3), 4.10~4.12(m, 2H, CH_2), 5.07(s, 2H, $ArCH_2O$), 5.53(m, 1H, CH), 7.35(s, 5H, ArH), 7.67(t, *J*=7.9 Hz, 1H, ArH), 7.89(d, *J*=7.3 Hz, 1H, ArH,), 8.20(d, *J*=8.2 Hz, 1H, -CONH-), 8.32(s, 1H, ArH), 8.50(d, *J*=7.6 Hz, 1H, ArH); **^{13}C NMR** (DMSO-d_6, 75 MHz) ***δ:*** 14.3, 57.6, 61.8, 66.3, 123.0, 123.5, 128.2, 128.3, 128.8, 130.5, 135.2, 137.1, 139.2, 148.2, 156.3, 170.3.

M6c: Propyl (S)-2-(benzyloxy)carbony)lamino)-2-(3-nitrophenyl)acetate

Yield 88%, m.p.: 106~107℃. **^{1}H NMR** (DMSO-d_6, 300 MHz) ***δ:*** 0.77(t, *J*=6.9 Hz, 3H, CH_3), 1.48~1.53(m, 2H, CH_2), 4.04(s, 2H, OCH_2), 5.09(s, 2H, $ArCH_2O$), 5.57(d, *J*=7.5Hz, 1H, CH), 7.36(s, 5H, ArH), 7.66~7.71(m, 1H, ArH), 7.91(d, *J*=7.2 Hz, 1H, ArH), 8.21(d, J=8.1 Hz, 1H, -CONH-), 8.35(s, 1H, ArH), 8.52(d, *J*=7.5 Hz, 1H, ArH); **^{13}C NMR** (DMSO-d_6, 75 MHz) ***δ:*** 10.4, 21.8, 57.6, 66.3, 67.1, 123.0, 123.5, 128.2, 128.3, 128.8, 130.4, 135.2, 137.1, 139.3, 148.1, 156.3, 170.3.

M6d: Butyl (S)-2-(benzyloxycarbonylamino)-2-(3-nitrophenyl)acetate

Yield 88%, m.p.: 132~133℃. **^{1}H NMR** (DMSO-d_6, 300 MHz) ***δ:*** 0.79(t, J_1=7.2 Hz, 3H, CH_3), 1.16~1.23 (m, 2H, CH_2), 1.46~1.50(m, 2H, CH_2), 4.05~4.09(m, 2H, OCH_2), 5.06(s, 2H, $ArCH_2O$), 5.56(d, *J*=8.1 Hz, 1H, CH), 7.37(s, 5H, ArH), 7.66~7.71(m, 1H, ArH), 7.91(d, *J*=7.5 Hz, 1H, ArH), 8.21(d, *J*=8.4 Hz, 1H, -CONH-), 8.35(s, 1H, ArH), 8.52(d, *J*=8.1 Hz, 1H, ArH); **^{13}C NMR** (DMSO-d_6, 75 MHz) ***δ:*** 13.8, 18.8, 30.4, 57.6, 65.4, 66.3, 123.0, 123.5, 128.2, 128.3, 128.8, 130.4, 135.2, 137.1, 139.3, 148.1, 156.3, 170.3.

M6e: Benzyl (S)-(2-((methylamino)oxy)-1-(3-nitrophenyl)-2-oxoethyl)carbamate

Yield 90%, m.p.: 113~114℃. **^{1}H NMR** (DMSO-d_6, 300 MHz) ***δ:*** 2.59(d, *J*=4.2 Hz, 3H, CH_3), 5.04(s, 2H, $ArCH_2O$), 5.38(d, *J*= 7.8 Hz, 1H, CH), 7.36(s, 5H, ArH), 7.62~7.70(m, 2H, ArH), 7.87(d, *J*=7.5 Hz, 1H, -CONH-), 8.15~8.25(m, *J*= 8.4 Hz, 2H, ArH), 8.33(d, 1H, -CONH-). **^{13}C NMR** (DMSO-d_6, 75 MHz) ***δ:*** 33.8, 57.9, 66.1, 122.4,

123.8, 128.1, 128.2, 128.7, 128.9, 130.3, 134.4, 137.2, 137.3, 148.1, 156.1, 169.7.

M6f: Benzyl (S)-(2-((ethylamino)oxy)-1-(3-nitrophenyl)-2-oxoethyl)carbamate

Yield 88%, m.p.: 116~117℃. **^{1}H NMR** (DMSO-d_6, 300 MHz) ***δ:*** 0.99(t, *J*=7.2 Hz, 3H, CH_3), 3.03~3.13(m, 2H, CH_2), 5.04(s, 2H, $ArCH_2O$), 5.38(d, *J*=8.4 Hz, 1H, CH), 7.31~7.37(m, 5H, ArH), 7.62~7.68(m, 1H, ArH), 7.87(t, *J*=8.1 Hz, 1H, -CONH-), 8.15(d, *J*=8.6 Hz, 1H, ArH), 8.24(d, *J*=8.7 Hz, 1H, ArH), 8.33(s, 1H, ArH), 8.40(d, *J*=8.3 Hz, 1H, -CONH-). **^{13}C NMR** (DMSO-d_6, 75 MHz) ***δ:*** 12.1, 33.8, 57.9, 66.1, 122.4, 123.8, 128.1, 128.2, 128.7, 128.9, 130.3, 134.4, 137.2, 137.3, 148.1, 156.1, 169.7.

M6g: Benzyl (S)-(2-((hydroxyamino)oxy)-1-(3-nitrophenyl)-2-oxoethyl)carbamate

Yield 67%, m.p.: 125~126℃. **^{1}H NMR** (DMSO-d_6, 300 MHz) ***δ:*** 5.04(s, 2H, CH_2), 5.30(d, *J*=8.4 Hz, H, CH), 7.36(s, 5H, ArH), 7.65~7.71(m, *J*=7.8 Hz, H, ArH), 7.88(d, *J*=7.8 Hz, H, NH), 8.16~8.25(dd, *J*=8.4, 9.6 Hz, H, ArH), 8.38(t, *J*=8.7 Hz, 2H, ArH), 9.13(s, H, NH), 11.08(s, H, OH). **^{13}C NMR** (DMSO-d_6, 75 MHz) ***δ:*** 55.8, 66.2, 122.2, 123.2, 124.0, 128.1, 128.3, 128.8, 130.4, 134.3, 137.2, 141.1, 148.1, 156.1.

M6h: Benzyl (S)-(2-(((2-hydroxyethyl)(methyl)amino)oxy)-1-(3-nitrophenyl)-2-oxoethyl)carbamate

Yield 86%, m.p.: 133~135℃, $[\alpha]_D^{20}$ +39.8(*c*=1.0 mg/mL, EtOAc); **^{1}H NMR** (DMSO-d_6, 300 MHz) ***δ:*** 2.87~2.99(m, 4H, $N(CH_3)\mathbf{CH_2}CH_2OH$ and $N(CH_3)CH_2\mathbf{CH_2}OH$), 3.51~3.52(m, 3H, CH_3), 5.04(s, 2H, $ArCH_2O$), 5.79~5.96(dd, *J*=7.8, 7.8 Hz, 1H, CH), 7.35(s, 4H, ArH), 7.67 (d, *J*=6.0 Hz, 1H, ArH), 7.85(d, *J*=7.2 Hz, 1H, ArH), 8.10(d, *J*=8.1 Hz, 1H, -CONH-), 8.16~8.23(m, 2H, ArH), 8.27 (s, 1H, ArH). **^{13}C NMR** (DMSO-d_6, 75 MHz) ***δ:*** 36.4, 54.5, 55.2, 58.8, 66.2, 123.0, 123.9, 128.1, 128.3, 128.8, 129.6, 135.1, 137.2, 155.9, 169.0, 169.6.

4.2.9 Preparation of TM4b~TM4h

The mixture of **M6** (1.0 mmol), Zn powder (11.0 mmol), NH_4Cl (6.0 mmol) and MeOH (15 mL) was stirred at 75~85 ℃ and monitored by TLC until completion. After hot filtration and washing residue with MeOH (2×2 mL), the filtrate was concentrated under reduced pressure to obtain the crude product.

The mixture of the crude product (0.9 mmol), dried acetone (5 mL) and K_2CO_3 (2.7 mmol) were added into the 50 mL round bottom flask. While the resultant mixture was stirred in an ice bath, the acetone solution (3 mL) of chloroacetyl chloride (0.97 mmol) was dripped slowly from the constant pressure funnel. After 5 min, removed the ice bath, stirred the reaction solution at 15℃-18℃ and monitored the reaction process by TLC until completion. Filtered by suction and washed the residue with acetone. The filtrate was concentrated under reduced pressure to obtain crude product, and followed the purification by silica gel column chromatography to obtain the pure **TM4b~TM4h**.

TM4b: Ethyl (S)-2-(benzyloxycarbonylamino)-2-(3-(2-chloroacetamido)phenyl)acetate

Yield 65%, m.p.: 83~84℃. **^{1}H NMR** (DMSO-d_6, 300 MHz) ***δ:*** 1.13(t, *J*=6.9 Hz, 3H, CH_3), 4.06~4.13(m, 2H, CH_2), 4.25(s, 2H, $COCH_2Cl$), 5.07(s, 2H, $ArCH_2O$), 5.21(d, *J*=7.5 Hz, 1H, CH), 7.12(s, 1H, ArH), 7.30~ 7.36(m, 6H, ArH), 7.59(d, *J*=6.6 Hz, 2H, ArH), 8.28(d, *J*=7.5 Hz, 1H, -CONH-), 10.38(s, 1H, -CONH-); **^{13}C NMR** (DMSO-d_6, 75 MHz) ***δ:*** 14.4, 44.0, 58.5, 61.4, 66.1, 119.2, 119.6, 123.6, 128.2, 128.3, 128.8, 129.5, 137.3, 137.4, 139.1, 156.1, 165.1, 170.9; **HRMS** calcd for $C_{20}H_{21}ClN_2O_5[M-H]^-$ 403.1066, found 403.1072.

TM4c: Propyl (S)-(benzyloxycarbonylamino)-2-(3-(2-chloroacetamido)phenyl)acetate

Yield 70%, m.p.: 95~96℃. **^{1}H NMR** (DMSO-d_6, 300 MHz) ***δ:*** 0.74~0.79(m, 3H, CH_3), 1.49~1.56(m, 2H, CH_2), 4.02(t, *J*=6.0 Hz, 2H, OCH_2), 4.25(s, 2H, CH_2Cl), 5.07(s, 2H, $ArCH_2O$), 5.22(d, J=7.2 Hz, 1H, CH), 7.14(d, *J*=7.5 Hz, 1H, ArH), 7.31~7.36(m, 6H, ArH), 7.58(d, *J*=14.1 Hz, 1H, ArH), 8.29(d, *J*=7.5 Hz, 1H, -CONH-), 10.39(s, 1H, -CONH-); **^{13}C NMR** (DMSO-d_6, 75 MHz) ***δ:*** 10.4, 21.8, 44.0, 58.3, 66.1, 66.8, 119.6, 128.1, 128.3, 128.7, 129.5, 137.2, 137.4, 139.0, 156.4, 165.1, 170.9. **HRMS** calcd for $C_{21}H_{23}ClN_2O_5$ [M-H]$^-$ 417.1223，found 417.1221.

TM4d: Butyl (S)-2-(benzyloxycarbonylamino)-2-(3-(2-chloroacetamido)phenyl)acetate

Yield 62%, m.p.: 114~115℃. **^{1}H NMR** (DMSO-d_6, 300 MHz) ***δ:*** 0.77~0.82(t, *J*=7.5 Hz, 3H, CH_3) , 1.16~ 1.26(m, 2H, CH_3**CH_2**), 1.44~1.53(m, 2H, CH_3CH_2**CH_2**), 4.04~4.08(m, 2H, OCH_2), 4.25(s, 2H, CH_2Cl), 5.11(s, 2H, $ArCH_2O$), 5.21(d, *J*=4.2 Hz, 1H, CH), 7.12(d, *J*=7.8 Hz, 1H, ArH), 7.30~7.36(m, 5H, ArH), 7.59(s, 1H, ArH), 8.28 (d, *J*=7.5 Hz, 1H, -CONH-), 10.38(s, 1H, -CONH-); **^{13}C NMR** (DMSO-d_6, 75 MHz) ***δ:*** 13.9, 18.2, 30.4, 44.0, 58.6, 65.0, 66.1, 119.2, 119.5, 123.6, 128.2, 128.3, 129.5, 137.3, 139.1, 156.3, 165.1, 171.0. **HRMS** calcd for $C_{22}H_{25}ClN_2O_5$**[**M-H]$^-$ 431.1379，found 431.1376.

TM4e: Benzyl (S)-(1-(3-(2-chloroacetamido)phenyl)-2-(methyl amino)-2-oxoethyl)carbamate

Yield 27%, m.p.: 101~102℃. **^{1}H NMR** (DMSO-d_6, 300 MHz) ***δ:*** 2.58(d, *J*=4.2 Hz, 3H, CH_3), 4.24(s, 2H, CH_2Cl), 5.03(s, 2H, $ArCH_2O$), 5.15(d, *J*=7.8 Hz, 1H, CH), 7.12(d, *J*=7.8 Hz, 1H, ArH), 7.26~7.35(m, 6H, ArH), 7.54~7.58(m, 2H, ArH), 7.85(d, *J*=8.1 Hz, 1H, ArH), 8.18(d, *J*=4.5 Hz, 1H, -CONH-), 10.35(s, 1H, -CONH-); **^{13}C NMR** (DMSO-d_6, 75 MHz) ***δ:*** 26.1, 44.0, 58.4, 65.8, 118.8, 119.1, 119.7, 123.3, 128.2, 128.8, 129.2, 134.5, 138.8, 139.9, 156.0, 165.1, 170.1. **HRMS** calcd for $C_{19}H_{20}ClN_3O_5$**[**M-H]$^-$ 404.1013，found 404.1016.

TM4f: Benzyl (S)-(1-(3-(2-chloroacetamido)phenyl)-2-(ethylamino)-2-oxoethyl)carbamate

Yield 46%, m.p.: 179~181℃. **^{1}H NMR** (DMSO-d_6, 300 MHz) ***δ:*** 1.00(t, *J*=7.2 Hz, 3H, CH_3), 3.02~3.10(m, 2H, -CH_2-), 4.26(s, 2H, CH_2Cl), 5.03(s, 2H, $ArCH_2O$), 5.15(d, *J*=7.8 Hz, 1H, CH), 7.12(d, *J*=7.8 Hz, 1H, ArH), 7.26~7.37(m, 6H, ArH), 7.55~7.58(m, 2H, ArH), 7.81(d, *J*=8.7 Hz, 1H, ArH), 8.26(d, *J*=8.4 Hz, 1H, -CONH-), 10.26(s, 1H, -CONH-,); **^{13}C NMR** (DMSO-d_6, 75 MHz) ***δ:***14.9, 34.0, 44.0, 58.8, 66.0, 118.7, 119.1, 123.1, 128.1, 128.2, 129.2, 137.3, 140.0, 156.2, 165.1, 169.6. **HRMS** calcd for $C_{20}H_{22}ClN_3O_5$**[**M-H]$^-$ 418.1170，found 418.1173.

TM4g: Benzyl (S)-(1-(3-(2-chloroacetamido)phenyl)-2-((hydroxyamino)oxy)-2-oxoethyl)carbamate

Yield 56%, m.p.: 103~105℃. **^{1}H NMR** (DMSO-d_6, 300 MHz) ***δ:*** 4.24(s, 2H, CH_2Cl), 5.04(s, 2H, $ArCH_2O$), 5.14(d, *J*=8.1, 1H, CH), 7.15(d, *J*=7.5, 1H, ArH), 7.21(s, 1H, ArH), 7.27~7.35(m, 5H, ArH), 7.56~7.60(m, 2H, Ar-H), 7.74(d, *J*=7.8, 1H, -CONH-), 10.35(s, 1H, -CONH-). **^{13}C NMR** (DMSO-d_6, 75 MHz) ***δ:*** 42.6, 55.8, 66.2, 122.2, 123.2, 124.0, 128.1, 128.3, 128.8, 130.4, 134.3, 137.2, 141.1, 148.1, 156.1, 165.4. **HRMS** calcd for $C_{18}H_{18}ClN_3O_6$**[**M-H]$^-$ 406.0806，found 406.0810.

TM4h: Benzyl (S)-(1-(3-(2-chloroacetamido)phenyl)-2-(((2-hydroxyethyl)(methyl)amino)oxy)-2-oxo ethyl)carbamate

Yield 38%, m.p.:103~104℃. **^{1}H NMR** (DMSO-d_6, 300 MHz) ***δ:***2.85~2.91(m, 4H, N(CH_3)**CH_2** CH_2OH and N(CH_3)CH_2**CH_2**OH), 3.45~3.48(m, 3H, CH_3), 4.24(s, 2H, $COCH_2Cl$), 5.02(s, 2H, $ArCH_2O$), 5.52~5.67(dd, *J*=7.8, 7.8 Hz, 1H, CH), 7.09(d, *J*=7.5, 1H, ArH), 7.29~7.34(m, 6H, ArH), 7.51 (d, *J*=7.2 Hz, 1H, ArH), 7.60~7.65(m, 1H, ArH), 7.69(s, *J*=7.5 Hz, 1H, -CONH-), 10.37(s, 1H, -CONH-); **^{13}C NMR** (DMSO-d_6, 75 MHz) ***δ:*** 34.4, 36.2, 44.0, 49.1, 50.2, 58.8, 66.0, 119.0, 124.0, 128.1, 128.2, 128.8, 129.5, 137.4, 139.1, 139.2, 156.1, 165.1, 170.0; **HRMS** calcd for $C_{21}H_{24}ClN_3O_6$ $[M-H]^-$ 448.1275，found 448.1278.

4.2.10 Preparation of M7 and TM4a

M2 (6.3 mmol), Zn powder (69.2 mmol), $CaCl_2$ (5.0 mmol), and the water solution of 95% EtOH (16 mL, volume ratio 4:1) were added into a 50 mL round bottom flask. Stirred and refluxed continuously at 80 ℃. The reaction progress was monitored by TLC. Upon completion, the solid was collected by filtration. The obtained solid was washed with EtOH (3 × 10 mL), the combined filtrate was concentrated under reduced pressure to obtain crude product. Subsequently, the crude product was washed thoroughly with water (3 x 5 mL), and then dried in vacuo overnight to afford the pure **M7**.

Synthesis of **TM4a**: **M7** (5.1 mmol), DCM (15 mL), anhydrous K_2CO_3 (36.4 mmol) was added into a 50 mL round bottom flask. While the mixture was stirred in an ice bath, the solution of chloroacetyl chloride (10.1 mmol) in DCM (5 mL) was dripped slowly from the constant pressure funnel. Then the mixture was stirred at ambient temperature and monitored by TLC. On completion of the reaction, cool saturated brine (20 mL) was added, the solid was subsequently collected by filtration. The filter cake obtained was dried overnight to afford the crude product, further recrystallization from mixed solvent of acetone and chloroform (6 mL, volume ratio 1:1) affords analytically pure **TM4a.**

M7: (S)-2-(((benzyloxy)carbonyl)amino)-2-(3-nitrophenyl)acetic acid

Yield 71%, m.p.: 77~78℃, $[\alpha]_D^{20}$ +81.36(c 2.2 mg/mL, DMF). **^{1}H NMR** (DMSO-d_6, 300 MHz) ***δ:***4.68(s, 1H, CH), 4.90(s, 2H, NH_2), 5.03(s, 2H, CH_2), 6.38(d, J_1=7.5 Hz, 2H ArH), 6.43~7.34(m, 7H, ArH); **^{13}C NMR** (DMSO-d_6, 75 MHz) ***δ:*** 57.9, 65.5, 113.6, 115.0, 121.5, 127.7, 127.8, 128.4, 129.0, 137.0, 137.5, 151.9, 155.9, 172.2.

TM4a: Potassium (S)-2-(((benzyloxy)carbonyl)amino)-2-(3-(2-chloroacetamido)phenyl)acetate

Yield 57%, m.p.: 79~80℃. **^{1}H NMR** (DMSO-d_6, 300 MHz) ***δ:***4.25(s, 1H, CH_2), 5.08(d, *J*=7.5 Hz, 2H, CH_2), 5.25(s, 1H, CH), 7.12(d, *J*=7.5 Hz, 1H, ArH), 7.33(t, *J*=8.4 Hz, 6H, ArH), 7.63(d, *J*=8.6 Hz, 2H, ArH), 8.32(d, *J*=8.4 Hz, 1H, NH), 10.40(s, 1H, NH); **^{13}C NMR** (DMSO-d_6, 75 MHz) ***δ:*** 43.6, 58.0, 65.8, 118.8, 119.3, 123.3, 127.8, 127.9, 128.4, 129.2, 136.9, 137.0, 138.7, 155.9, 164.8, 171.1. **HRMS** calcd for $C_{18}H_{16}ClKN_2O_5$ $[M-H]^-$ 413.0307，found 413.0310.

4.3. Biology

4.3.1 The determination of *α*-glucosidase inhibition [16]

α-Glucosidase inhibitory activity was determined in a 100 μL reaction mixer containing optimal rat-α-glucosidase(extracted from the rat small intestine of rat), 67 mmol L^{-1} pH 6.8 sodium phosphate buffer and

different samples. Blank control (without enzyme and samples) or negative control (without sample) was set as above. After incubation at 37 ℃ for 10 min, 0.1 mol L^{-1} maltose was added and incubated for another 10 min at room temperature. The reaction was stopped with 200 μL of glucose and the optical density (OD) values at 490 nm recorded. The inhibition ratio was calculated according to the following equation: $I\%= [1-(OD_{Sample}-OD_{Blank}) / (OD_{Negative}-OD_{Blank})] \times 100\%$. Based on the inhibition value, IC_{50} was calculated using the 4 Parameter Logistic Model in Xlfit. For each concentration of each sample in duplicate was performed and repeated once.

4.3.2 Inspection and Test of PPAR activation [16]

HepG2 cells were cultured in low glucose Dulbecco's Modified Eagle's medium (DMEM) supplemented with 100 U mL^{-1} streptomycin and penicillin. One day prior to transfection, the cells were plated in 96-well plates with 1.5×10^4 cells per well. When the cells grew at a confluence of 70%, plasmid pPPRE-Luc with firefly luciferase reporter gene and the control plasmid phRL-TK with Renilla luciferase reporter gene were transfected into the cells. 24 hours after the transfection, the medium was replaced with fresh medium containing either different samples, rosiglitazone (positive control) or without sample (negative control). The cells without transfection were used as a blank control. After incubation for a further 24 h, the expression of luciferases was measured with a Dual-Luciferase Reporter Gene Assay Kit (Promega). The times the samples became activated (T%) were calculated as the following equation: $T = [(L1_{Sample} - L1_{Blank}) / (L1_{Negative} - L1_{Blank})] / [(L2_{Sample} - L2_{Blank}) / (L2_{Negative} - L2_{Blank})] \times 100\%$. Here, L_1 represents the values for firefly luciferase and L_2 represents the values for Renilla luciferase. For each concentration of each sample in duplicate was performed and repeated once.

4.3.3 The determination of dipeptidyl peptidase-IV (DPP-IV) [48]

The reaction system of 200 μL containing the DPP-IV (Sigma) and 25 mmol/L HEPES buffer (140 mmol/L NaCl, 1% BSA, 80 mmol/L $MgCl_2$) incubated for 10 min at room temperature while blank control (without enzyme and the sample) and negative control (without sample) existed at the same condition, followed by dipeptidyl peptidase GLY-PRO-GLY-GLY added. After incubation at room temperature for 25-40min, fluorescence strength F was measured under excitation wavelength of 355 nm and emission wavelength of 460 nm. The samples inhibition ratio were calculated as the following equation: $I\%= [1-(F_{sample}-F_{blank})/ (F_{negative}-F_{blank})]\times 100$ %. Based on the inhibition value, IC_{50} was calculated using 4 Parameter Logistic Model in Xlfit. For each concentration of each sample in duplicate was performed and repeated once.

Acknowledement

The authors are grateful to Prof. Qunli Luo and Mr. Ning Wang for their assistance in measuring ^{1}H NMR and ^{13}CNMR spectra. We thank the Scientific and Technological Project in Chongqing (CSTC, 2011AB 5001)，the Natural Science Foundation of Chongqing (CSTC,2016jcyjA0421), The National Natural Science Foundation of China (NSFC, nos. 21542003) for financial support.

Reference

[1] World Health Organization. Global report on diabetes. http://www.who.int/diabetes/global-report/en/; 2016 accessed 26 August 2017.

[2] Xu SS, Zhang HB, Zhou JP, et al. Advances of new antidiabetic drugs. *J China Pharm Univ*. 2011;42: 97-106.
[3] Garcia-Vallvé S, Guasch L, Tomas-Hernández S, et al. Peroxisome proliferator-activated receptor γ (PPARγ) and ligand choreography: Newcomers take the stage. *J Med Chem*. 2015;58:5381-5394.
[4] Hallenborg P, Petersen RK, Kouskoumvekaki I, et al. The elusive endogenous adipogenic PPARγ agonists: Lining up the suspects. *Prog Lipid Res*. 2016;61:149-162.
[5] Choi JH, Banks AS, Estall JL, et al. Anti-diabetic drugs inhibit obesity-linked phosphorylation of PPARgamma by Cdk5. *Nature*. 2010;466:451-456.
[6] Yasmin S, Jayaprakash V. Thiazolidinediones and PPAR orchestra as antidiabetic agents: From past to present. *Eur J Med Chem*. 2017;27:879-893.
[7] Rizos CV, Kei A, Elisaf MS. The current role of thiazolidinediones in diabetes management. *Arch Toxicol*. 2016;90:1861-1881.
[8] Sun ZS. Oral antidiabetic drug—nateglinide. *J Pract Diabet*. 2006;2:53-54.
[9] Gopi G, Kannan K, Manavalan R. Seletion of excipients for nanoparticles formulations of nateglinide through drug-excipients compatibility study. *Int J Pharma Pharmac Sci*. 2013;5:371-377.
[10] Pari L, Ashokkumar N. Effect of *N*-benzoyl-D-phenylalanine, a new potential oral antidiabetic agent, in neonatal streptozotocin-induced diabetes in rats. *Pharmacol Rep*. 2005;57:498-503.
[11] Henke BR, Blanchard SG, Brackeen MF, et al. N-(2-benzoylphenyl)-L-tyrosine PPARγ agonists. 1. Discovery of a novel series of potent antihyperglycemic and antihyperlipidemicagents. *J Med Chem*. 1998;41:5020-5036.
[12] Ciantar J, Shoemake C, Mangani C, et al. Optimisation of tyrosine-based lead molecules capable of modulation of the preroxisome proliferator-activated receptor gamma. *IJPSR*. 2012;3:2550-2561.
[13] Pirat C, Farce A, Gue NL, et al. Targeting peroxisome proliferator-activated receptors (PPARs): Development of Modulators. *J Med Chem*. 2012;55:4027-4061.
[14] Ma Y, Wang SQ, Xu WR, et al. Design novel dual agonists for treating type-2 diabetes by targeting peroxisome proliferator-activated receptors with core hopping approach. *PLoS One*. 2012;7:e38546.
[15] Cobb JE, Blanchard SG, Boswell EG, et al. *N*-(2-Benzoylphenyl)-L-tyrosine PPARγ agonists. 3. Structure-activity relationship and optimization of the *N*-aryl substituent. *J Med Chem*. 1998;41:5055 -5069.
[16] Tang GX, Yan JF, Fan L, et al. Synthesis of novel *β*-amino ketones containing a *p*-aminobenzoic acid moiety and evaluation of their antidiabetic activities. *Sci China Chem*. 2013;56:490-504.
[17] Meng Y, Hu WX, Wang LG. Preparation of chlorophenylglycineas phamaceutical intermediate. *Zhejiang Chem Ind*. 2006;37:24-26.
[18] Titulaer GTM, Zhu J, Klunder AJH, et al. A new synthesis of *p*-hydroxy phenylglycine and some snalogues from *p*-benzoquinone. *Org Lett*. 2000;2:473-475.
[19] Cronet P, Petersen JFW, Folmer R, et al. Structure of the PPARα and -γ ligand binding domain in complex with AZ 242; ligand selectivity and agonist activation in the PPAR family. *Structure*. 2001;9: 699-706.
[20] Suh YG, Kim NJ, Koo BW, et al. Design, synthesis, and biological evaluation of novel constrained meta-substituted phenyl propanoic acids as peroxisome proliferator-activated receptor α and γ dual agonists. *J Med Chem*. 2008;51:6318-6333.
[21] Khanna S, Sobhia ME, Bharatam PV. Additivity of molecular fields: CoMFA study on dual activators of PPARα and PPARγ. *J Med Chem*. 2005;48:3015-3025.
[22] Davidson MA, Mattison DR, Azoulay L, et al. Thiazolidinedione drugs in the treatment of type 2 diabetes mellitus: past, present and future. *Crit Rev Toxicol*. 2017;48:58-108.
[23] Machado AL, Lima LM, Araújo-Jr JX, et al. Design, synthesis and antiinflammatory activity of novel phthalimide derivatives, structurally related to thalidomide. *Bioorg Med Chem Lett*. 2005;15:1169- 1172.
[24] Gobec S, Plantan I, Mravljak J, et al. Design, synthesis, biochemical evaluation and antimycobacterial action of phosphonate inhibitors of antigen 85C, a crucial enzyme involved in biosynthesis of the mycobacterial cell wall. *Eur J Med Chem*. 2007;42:54-63.

[25] Nagarajan S, Majumder S, Sharma U, et al. Synthesis and anti-angiogenic activity of benzothiazole, benzimidazole containing phthalimide derivatives. *Bioorg Med Chem Lett*. 2013;23:287-290.

[26] Su XY, Wang CL, Kong LQ, et al. Investigation on synthetic technology of *m*-nitro-*L*- phenylglycine, *J Southwest China Norm. Univ (Nat Sci)*. 2010;32:45-49.

[27] Li HC, Yan JF, Su XY, et al. Synthesis and antidiabetic activities of *L*-phenylglycine derivates, *Chin J Synth Chem*. 20111;9:441-445.

[28] Yang DC, Fan L, Su XY, et al. L-*m*-Aminophenylglycine and derivative thereof, preparation method and application thereof. ZL200910104610.5, 2013-01-30

[29] Sun XL, Fan L, Tang XM, et al. Application of thionyl chloride-alcohol system in organic synthesis. *J Org Chem Res*. 2016;4:23-32.

[30] Yang DC, Fan L, Hong YG. Synthesis of protected RGD tripeptide. *Chin J Org Chem*. 2003;23: 493-498.

[31] Yang Y, Yan JF, Fan L, et al. Synthesis and PPAR activities of novel phenylacetic acid derivatives containing sulfonamide moiety. *Acta Pharm Sin*. 2012;47:1630-1639.

[32] Yang L, Yan JF, Fan L, et al. Synthesis and antidiabetic activity of novel molecules containing *p*-aminobenzoic acid and benzenesulfonamide moiety. *Chin J Org Chem*. 2012;32:1908-1918.

[33] Han L, Shen WJ, Bittner S, et al. PPARs: regulators of metabolism and as therapeutic targets in cardiovascular disease. Part II: PPAR-*β*/*δ* and PPAR-*γ*. *Future Cardiol*. 2017;13:279-296.

[34] Ryu S, Kim DS, Lee MW, et al. Anti-leukemic effects of PPAR*γ* ligands. *Cancer Lett*. 2018;418:10-19.

[35] Zhang J, Liu X, Xie XB, et al. Multitargeted bioactive ligands for PPARs discovered in the last decade. *Chem Biol Durg Des*. 2016;88:635-663.

[36] Rengasamy KRR, Aderogba MA, Amoo SO, et al. Potential antiradical and alpha-glucosidase inhibitors from Ecklonia maxima (Osbeck) Papenfuss. *Food Chem*. 2013;141:1412-1415.

[37] Zheng TP, Yang F, Gao Y, A. et al. Increased plasma DPP4 activities predict new-onset atherosclerosis in association with its proinflammatory effects in Chinese over a four year period: A prospective study. *Atherosclerosis*. 2014;235:619-624.

[38] Xiao PF, Guo R, Huang SQ, et al. Discovery of dipeptidyl peptidase IV (DPP4) inhibitors based on a novel indole scaffold. *Chin Chem Lett*. 2014;25:673-676.

[39] Barakat1 GM, Nuwayri-Salti N, Kadi LN, et al. Role of glucagon-like peptide-1 and its agonists on early prevention of cardiac remodeling in type 1 diabetic rat hearts. *Gen Physiol Biophys*. 2011;30:34-44.

[40] Kim KR, Rhee SD, Kim HY, et al. KR-62436, 6-{2-[2-(5-cyano-4,5-dihydropyrazol-1-yl)-2–oxo-ethylamino]ethylamino}nicotinonitrile, is a novel dipeptidyl peptidase-IV (DPP-IV) inhibitor with anti-hyperglycemic activity. *Eur J Pharm*. 2005;518:63-70.

[41] Zhang HZ, Damu GL, Cai GX, et al. Design, synthesis and antimicrobial evaluation of novel benzimidazole type of Fluconazole analogues and their synergistic effects with Chloromycin, Norfloxacin and Fluconazole. *Eur J Med Chem*. 2013;64:329-344.

[42] Dai LL, Zhang HZ, Nagarajan S, et al. Synthesis of tetrazole compounds as a novel type of potential antimicrobial agents and their synergistic effects with clinical drugs and interactions with calf thymus DNA. *Med Chem Commun*. 2015;6:147-154.

[43] Brullo C, Ricciarelli R, Prickaerts J, et al. New insights into selective PDE4D inhibitors: 3-(Cyclopentyloxy)-4-methoxybenzaldehyde O-(2-(2,6-dimethylmorpholino)-2-oxoethyl)oxime (GEBR-7b) structural development and promising activities to restore memory impairment. *Eur J Med Chem*. 2016;124:82-102.

[44] Lu SY, Jessen B, Strock C, et al. The contribution of physicochemical properties to multiple in vitro cytotoxicity endpoints. *Toxicol in Vitro*. 2012;26:613-620.

[45] Lipinski CA, Lombardo F, Dominy BW, et al. Experimental and computational approaches to estimate solubility and permeability in drug discovery and development settings. *Adv Drug Deliv Rev*. 2001;46: 3–26.

[46] Bikker J, Humblet C. Escape from flatland: Increasing saturation as an approach to improving clinical success. *J Med Chem*. 2009;52:6752–6756.

[47] Veber DF, Johnson SR, Cheng HY, et al. Molecular properties that influence the oral bioavailability of drug candidates. *J Med Chem*. 2002;45:2615-2623.

[48] Zhang XH, Yan JF, Fan L, et al. Synthesis and antidiabetic activity of *β*-acetamido ketones. *Acta Pharm Sin B.* 2011;1:100-105.

Highlights

- Obtained 28 L-phenylglycine derivatives by two rounds of design and synthesis.
- Tested peroxisome proliferator-activated receptor activated activity, α-glucosidase inhibitory and DPP-4 inhibitory activities.
- **TM4h** possessed the most potent PPRE relative activity.
- Tentatively evaluated the lead-likeness and safety by physical parameter calculation and toxicity prediction.

Graphical Abstract

To create your abstract, type over the instructions in the template box below.
Fonts or abstract dimensions should not be changed or altered.

Design, synthesis, and evaluation of novel L-phenylglycine derivatives as potential antidiabetic lead compounds

Leave this area blank for abstract info.

Liu Jinyu [a], Su Xiaoyan [a], Li Huachong [a], Fan Li [a,*],
Li Yuanyuan [a],Tang Xuemei [b], Yan Jufang [c], Chen xin [c], Chen Feifei[a], Liu Jie[a], Yang Dacheng [a,*]

[a] *Institute of Bioorganic and Medicinal Chemistry, Key Laboratory of Applied Chemistry of Chongqing Municipality, School of Chemistry and Chemical Engineering, Southwest University, Chongqing 400715, PR China.*
[b] *School of Life Science, Southwest University, Chongqing 400715, China*
[c] *Drug Screening Center, Chengdu Di Ao Pharmaceutical Group Co., Ltd., Chengdu 610041, China*